

# Oxymatrine inhibits the development of radioresistance in NSCLC cells by reversing EMT through the DcR3/AKT/GSK-3 $\beta$ pathway

Jianming Tang, Yu Cao, Hong Zhang, Rui Wang

The Third Affiliated Hospital of Chongqing Medical University, Chongqing, China

**Submitted:** 24 June 2022; **Accepted:** 24 December 2022

**Online publication:** 5 January 2023

Arch Med Sci

DOI: <https://doi.org/10.5114/aoms/158533>

Copyright © 2023 Termedia & Banach

**Corresponding author:**

Rui Wang PhD

The Third Affiliated Hospital

of Chongqing

Medical University

Chongqing, China

e-mail: [650614@hospital.cqmu.edu.cn](mailto:650614@hospital.cqmu.edu.cn)

## Abstract

**Introduction:** Lung cancer is the leading cause of cancer-associated mortality globally. In particular, non-small cell lung cancer (NSCLC) constitutes the largest percentage of all cases of lung cancer. In clinical practice, radioresistance contributes to poor responses to radiotherapy. Therefore, the demand remains to explore potential novel and effective mechanism underlying radioresistance to improve the efficacy of radiotherapy for NSCLC.

**Material and methods:** Western blotting was conducted to quantify the protein expression of epithelial-mesenchymal transition markers E-cadherin and vimentin in the A549 cell line. The proliferation of A549 cells was measured using the Cell Counting Kit-8 and colony forming assays. In addition, the apoptosis of A549 cells was analyzed by flow cytometry. Invasion and migration by NSCLC cells were quantified using Transwell and wound healing assays. Plasmids were used to overexpress decoy receptor 3 (DcR3) in A549 cells. Xenograft models were established to measure the extent of NSCLC tumor growth *in vivo*.

**Results:** Our study clarified the activation of the DcR3/protein kinase B (AKT)/glycogen synthase kinase 3 $\beta$  (GSK-3 $\beta$ ) pathway in radioresistant NSCLC cells. Oxymatrine (OMT) treatment restored radiosensitivity and inhibited irradiation-induced epithelial-mesenchymal transition (EMT), invasion and migration in NSCLC cells through the DcR3/AKT/GSK-3 $\beta$  pathway *in vitro*. By contrast, OMT treatment promoted the suppressive effects of radiation on the weight and volume of the xenograft tumors in animal models.

**Conclusions:** In conclusion, OMT suppressed the development of radioresistance in NSCLC cells by promoting radiosensitivity, through the reversal of EMT process by inhibiting the DcR3/AKT/GSK-3 $\beta$  pathway.

**Key words:** non-small cell lung cancer, oxymatrine, invasion, migration, A549 cell, xenograft.

## Introduction

Lung cancer is the leading cause of cancer-associated mortality globally [1]. In particular, non-small cell lung cancer (NSCLC) constitutes the largest histological subtype of lung cancer, accounting for > 80% of all cases of lung cancer [2]. It has been previously reported that radiotherapy confers a degree of clinical benefit on patients with NSCLC [3]. However, the majority of patients with NSCLC will eventually succumb to this disease despite undergoing radiotherapy. In addition, resistance to radiotherapy contributes to the poor prognosis. Therefore, it remains of

importance to unravel novel and effective mechanisms underlying radioresistance to improve the efficacy of radiotherapy for NSCLC.

Oxymatrine (OMT), a quinolizidine alkaloid that can be extracted from the roots of the traditional Chinese herb *Sophora flavescens* Aiton, has recently attracted the attention of the scientific community due to its therapeutic effects on a number of diseases [4]. During NSCLC pathogenesis, OMT has been found to function as a tumor suppressor. OMT has been found to suppress the activation of epidermal growth factor receptor (EGFR) signaling to inhibit the proliferation of NSCLC [5]. Additionally, OMT has been reported exert a protective effect against NSCLC development through upregulating miR-367-3p expression to downregulating serum/glucocorticoid-regulated kinase member 3 [6]. These emerging evidences suggests that OMT may exert protective impacts against NSCLC. however, the specific effects of OMT on NSCLC radioresistance remain unclear.

Decoy receptor 3 (DcR3), also known as TR6, M68 or tumor necrosis factor (TNF) receptor superfamily (TNFSR) member 6B, is a soluble receptor that is also part of the TNFSR family. DcR3 is a secreted protein that does not have transmembrane domains [7]. At present, three ligands of DcR3 have been discovered, including Fas ligand, TNF superfamily member 14 and TNF-like ligand 1A, which can suppress apoptosis, regulate the immune system and inhibit angiogenesis, respectively [7–9]. however, DcR3 is expressed at negligible levels in normal tissues, such that its aberrant expression has been reported to be associated with various types of malignancies. A previous clinical study of 365 cases has demonstrated that DcR3 may participate in the tumorigenesis and deterioration of lung cancer [10]. Despite this, the specific function of DcR3 in NSCLC remains poorly understood. Therefore, in this study we aim to clarify the function of DcR3 in the radiosensitivity of NSCLC and its EMT mechanism.

In the present study, we aimed to explore the impact of OMT treatment on the radiosensitivity of NSCLC. In addition, we planned to clarify the role of the DcR3/protein kinase B (AKT)/glycogen synthase kinase 3 $\beta$  (GSK-3 $\beta$ ) pathway in the radioresistance of NSCLC and irradiation-induced EMT in NSCLC cells. AKT signaling pathway plays an important role in the development of cancer. It was reported that Glucose fluctuation aggravates mesangial cell apoptosis, which may be partly induced by activating oxidative stress and inhibiting the AKT signaling pathway [11]. GSK-3 $\beta$  is involved in transcriptional activation, cell proliferation, cell differentiation and cell movement and other physiological processes [12]. Results from this study might indicate the effect and mech-

anism of OMT treatment on radiosensitivity of NSCLC cells. These findings may be beneficial for deepening the understanding into the effects of OMT treatment on radioresistance in NSCLC cells.

## Material and methods

### Experiment design

To investigate the effect of OMT treatment on radioresistance in NSCLC cells, we first established radioresistant A549 cells using an X-RAD 225 irradiator. Subsequently, we measured the expression of EMT proteins in A549 cells to see whether EMT was activated in radioresistant A549 cells. Next, we treated radioresistant A549 cells with OMT to see whether it restored the radiosensitivity of NSCLC cells by inhibiting cell colony formation, proliferation, EMT, invasion and migration and promoting cell apoptosis. To investigate the underlying mechanism of OMT treatment on radioresistance in NSCLC cells, we measured the changes of DcR3/AKT/GSK-3 $\beta$  signaling in radioresistant NSCLC cells. After we confirmed that DcR3/AKT/GSK-3 $\beta$  signaling was activated in radioresistant NSCLC cells, we inhibited the DcR3/AKT/GSK-3 $\beta$  signaling and examined effect of OMT treatment on the radiosensitivity, irradiation-induced EMT and invasion in NSCLC cells. Finally, we tested the effect of OMT on the tumor growth in radioresistant xenograft models.

### Cell culture

The A549 cell line was purchased from the Cell Bank of the Chinese Academy of Sciences and cultured in RPMI-1640 medium (Hyclone; Cytiva) supplemented with 10% FBS (#12483020, Gibco; Thermo Fisher Scientific, Inc., Cleveland, OH, USA). Cells were seeded into T-75 flasks and incubated under 5% CO<sub>2</sub> atmosphere at 37°C. OMT (purity  $\geq$  98%) and the AKT inhibitor MK-2206 were obtained from MedChemExpress (#HY-108232, Monmouth Junction, USA). In some experiments, A549 cells were treated with 2 mM OMT or 20  $\mu$ M MK-2206.

### Establishment of radioresistant A549 cells

To investigate the impact of OMT on the development of radioresistant NSCLC cells, we performed cell irradiation on the A549 cell lines using an X-RAD 225 irradiator. After  $\sim$ 12 days, we measured the proliferation of A549 cells using CCK-8 assays. We used an X-RAD 225 irradiator (Precision X-ray) to perform irradiation. Briefly, a dose of 2 Gy (3.2 Gy/min; 13.3 mA; 225 kV; 2-mm Al filter) radiation was delivered to A549 cells at 50% confluency at room temperature, before they were passaged in new flasks to  $\sim$ 80% confluence. Afterwards, this 2-Gy radiation was delivered re-

peatedly to the cells at 50% confluency until a cumulative dose of 60 Gy has been administered. In parallel, parental cells that were not irradiated were cultured and passaged simultaneously.

#### Procedures of siRNA treatment

A549 cells were transfected with the specific siRNA (DcR3 siRNA, Akt siRNA, or GSK-3 $\beta$  siRNA) using Transfection Reagent from TransGen Biotech, Co., Ltd. (China) following the manufacturer's instruction. The plasmid vector of pGCSi-U6-Neo-GFP-NegConshRNA was used as the negative control (NC siRNA). The RPMI 1640 medium with 5% FBS was changed to antibiotic-free growth media on day 1 of A549 cells. The next day, siRNA (50 nM) was transfected using Transfection Reagent. Six hours after transfection, RPMI 1640 containing 6% FBS was added to each well to a final concentration of 2% FBS. The interval between transfection and subsequent experimentation was 2 weeks.

#### Apoptosis assay

A549 cells were incubated in 96-well plates ( $1 \times 10^4$  cells/well), before they were treated with OMT or MK-2206 at final concentrations for 24 h. The cell apoptotic rate was quantified using an Annexin V-FITC Apoptosis Detection Kit (#KGA1014, Nanjing KeyGen Biotech Co., Ltd. Nanjing, China). Briefly, cells were harvested and stained with Annexin V-FITC (10  $\mu$ l) and propidium iodide (5  $\mu$ l). The degree of cell apoptosis was measured using the BD FACScan<sup>®</sup> flow cytometer (BD Biosciences, Inc., San Jose, CA, USA).

#### Cell viability assay

The cell viability of A549 cells was assessed using a Cell Counting Kit-8 (CCK-8) Assay (#ab228554, Abcam, Cambridge, MA, USA). Briefly, A549 cells were treated with OMT or MK-2206 at their final concentrations for 24 h. Each group of cell suspensions was then divided into 96-well plates ( $5 \times 10^4$  cells/ml) suspended in RPMI-1640 medium (Sigma, USA) for 24 h. We then changed the medium to a mixture of 90  $\mu$ l fresh medium containing 5  $\mu$ l of the CCK-8 solution. Subsequently, the 96-well plates were incubated for 2 h at room temperature, before the optical density value was measured in each well at 450 nm using a microplate reader (BioTek Instruments, Inc., Winooski, VT, USA; Agilent Technologies, Inc., Santa Clara, CA, USA).

#### Transwell assay

Cells were suspended in RPMI-1640 medium (Sigma, USA) and added at  $2 \times 10^4$  cells into an

insert (Corning, Inc., Corning, NY). First, we used Matrigel (Sigma-Aldrich; Merck KGaA, St. Louis, MO, USA) to precoat the upper membrane. The bottom of the chambers was then filled with 500  $\mu$ l RPMI-1640 medium containing 5% FBS (Gibco; Thermo Fisher Scientific, Inc., Cleveland, OH, USA) to be the chemoattractant. After 48 h, we used a cotton swab to wipe away the cells that did not invade. The invasive cells on the bottom of the chambers were then fixed using 8% paraformaldehyde. Visualization of the invasive cells was performed by staining the cells with 0.1% crystal violet followed by imaging under the microscope (Carl Zeiss AG, Jena, Germany).

#### Western blotting

Epithelial-mesenchymal transition is a process in which epithelial cells acquire the phenotype of mesenchymal stem cells, which has been reported to be associated with the development of drug resistance and tumor growth [13, 14]. To verify the effect of irradiation on NSCLC cells, we treated the A549 cells with different doses of irradiation (0, 10, 20, 30, 40 and 50 Gy) before evaluating the expression of EMT markers E-cadherin, N-cadherin, Vimentin, twist and snail1 in each group of cells. We used the radioimmunoprecipitation assay buffer (Sigma-Aldrich; Merck KGaA) to extract protein samples from the cultured cells or xenograft tumors. The proteins were separated using SDS-PAGE before being transferred onto PVDF membranes (Cytiva, USA). Specific primary antibodies were then incubated with the membranes at 4°C overnight. The following day, the membranes were washed three times and incubated with the secondary antibodies at room temperature for 2 h. Protein bands were visualized using chemiluminescence reagents (Absin Bioscience, Inc., Shanghai, China). Band intensities were quantified using the Image-Pro Plus 6.0 software (Media Cybernetics, Inc.). GAPDH was used for normalization. The antibodies used in this study were listed in Table 1.

#### Colony formation assay

For colony formation, A549 cells were cultured in an incubator containing 5% CO<sub>2</sub> at 37°C. The cells were then treated with either OMT or MK-2206 at final concentrations for 24 h. Afterwards, A549 cells were seeded into six-well plates (500 cells/well). After 2 weeks, the cells were fixed in 4% methanol and stained with 0.2% crystal violet, before the number of colonies formed was counted.

#### Wound healing assay

After cells were allowed to attach and grew to 90% confluency, a scratch was made through the confluent cell monolayer using a 200- $\mu$ l sterile pi-

**Table I.** Antibodies used in the study

Reagent	Source	Identifier
Primary antibodies:		
Anti-E-cadherin antibody, rabbit monoclonal	Abcam	ab40772
Anti-vimentin antibody, rabbit monoclonal	Abcam	ab92547
Anti-N-cadherin antibody, rabbit monoclonal	Abcam	ab76011
Anti-Twist, mouse monoclonal	Abcam	ab50887
Anti-Snail antibody, rabbit monoclonal	Abcam	a216347
Anti-DcR3 antibody, mouse monoclonal	Abcam	ab233816
Anti-Akt antibody, rabbit polyclonal	Cell signaling technology	#9272
Anti-Phospho-Akt antibody, rabbit monoclonal	Cell Signaling Technology	#4060
Anti-GSK-3 $\beta$ antibody, rabbit monoclonal	Cell Signaling Technology	#12456
Anti-Phospho-GSK-3 $\beta$ antibody, rabbit monoclonal	Cell Signaling Technology	#5558
Anti- $\beta$ -actin antibody, rabbit polyclonal	Affinity	AF7018
Secondary antibodies:		
Goat Anti-Rabbit IgG h&L (HRP)	Abcam	ab97051
Goat Anti-Rat IgG h&L (Alexa Fluor® 647)	Abcam	ab150167

pette tip. PBS was then used to wash away any suspended cells. Images were taken using an Axio Scope A1 optical microscope (Carl Zeiss AG, Jena, Germany) 0 and 24 h after wounding.

#### Cell transfection

The overexpression vectors for DcR3 were constructed by Shanghai GeneChem Co., Ltd. After the cell density reached 70–90%, the plasmids were transfected into the cells using the Lipofectamine 3000 reagent (Thermo Fisher Scientific, Inc., Cleveland, OH, USA). After 48 h, the cells were collected and treated with cell irradiation.

#### Animal experiments

BALB/c nude mice (4 weeks old) were purchased from the Experimental Animal Centre of The Third Affiliated hospital of Chongqing Medical University (Chongqing, China). The mice were cultured under specific-pathogen-free conditions. For xenograft tumor development, irradiation-resistant A549 cells were collected ( $1 \times 10^7$  cells in 100  $\mu$ l) and subcutaneously injected. We then measured the weight of tumor every 4 days. After 24 days, we euthanized the mice by CO<sub>2</sub> inhalation and pentobarbital sodium injection (i.p., 100 mg/kg) before collecting to evaluate their sizes. The samples were stored at  $-80^\circ\text{C}$  until further analysis. The entire experimental protocol adhered to the 'Guide for the Care and Use of Laboratory Animals, 8<sup>th</sup> edition.

#### Statistical analysis

All data were analyzed using the SPSS 21.0 Software (IBM Corp.). Data are presented as the mean

$\pm$  standard deviation.  $P < 0.05$  was considered to indicate a statistically significant difference.

## Results

### Establishment of the radioresistant NSCLC cells

Compared with that in normal A549 cells, cell viability was increased after irradiation treatment (Figure 1 A). Subsequently, we measured the expression of proliferative markers E-cadherin and Vimentin in A549 cells. The protein expression of E-cadherin was decreased whereas that of vimentin was increased in irradiated A549 cells (Figures 1 B, C).

We evaluated the expression of EMT markers E-cadherin, N-cadherin, vimentin, twist and snail1 in each group of cells. The results demonstrated that the protein expression of these markers was changed in a dose-dependent manner (Figures 1 D–G). Furthermore, we also utilized Transwell invasion and wound healing assays to assess the invasive and migratory capabilities of A549 cells. The invasion and migration of A549 cells were increased after cell irradiation (Figures 2 A–E).

### OMT treatment restores the radiosensitivity of NSCLC cells by inhibiting cell colony formation, proliferation and promoting cell apoptosis

After successfully establishing the radioresistant NSCLC cells, we investigated the effects of OMT treatment on the radiosensitivity of NSCLC cells. Firstly, we measured the degree of colony formation by the A549 cells using colony formation assay.

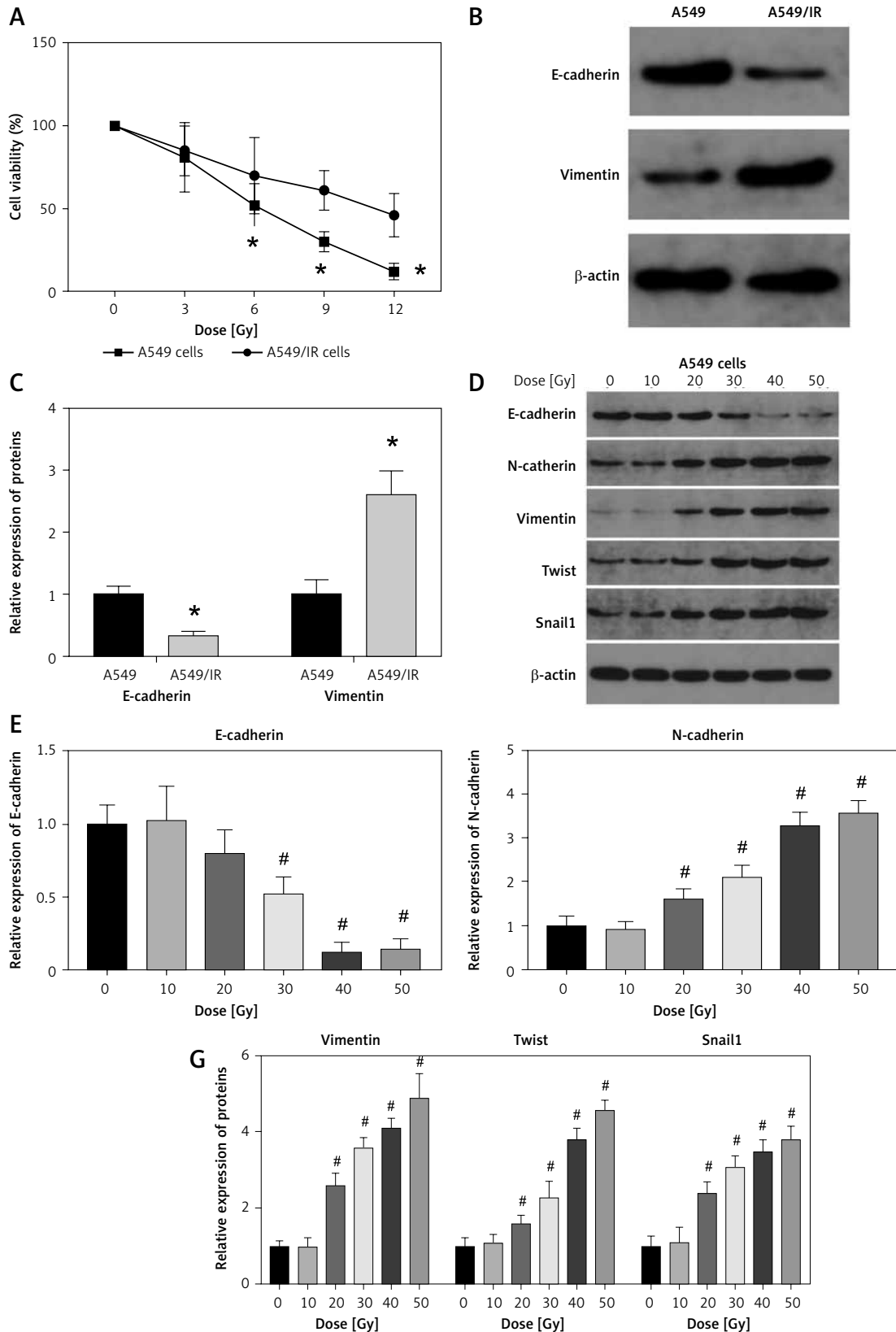


**Figure 1.** Establishment of radioresistant non-small-cell lung cancer cells. **A** – Viability of A549 cells after irradiation was analyzed using the Cell Counting Kit-8 assay. **B, C** – Protein expression of E-cadherin and Vimentin in A549 cells after irradiation.  $\beta$ -actin was used for normalization. **D–G** – The protein expression of epithelial-mesenchymal transition markers E-cadherin, N-cadherin, vimentin, twist and snail1 was measured after different doses of cell irradiation.  $\beta$ -actin was used for normalization. Each experiment was performed three times and the data are presented as the mean  $\pm$  standard deviation

\* $p < 0.05$  compared to A549 cell group. # $p < 0.05$  compared to 0 Gy group.  $N = 10$ .

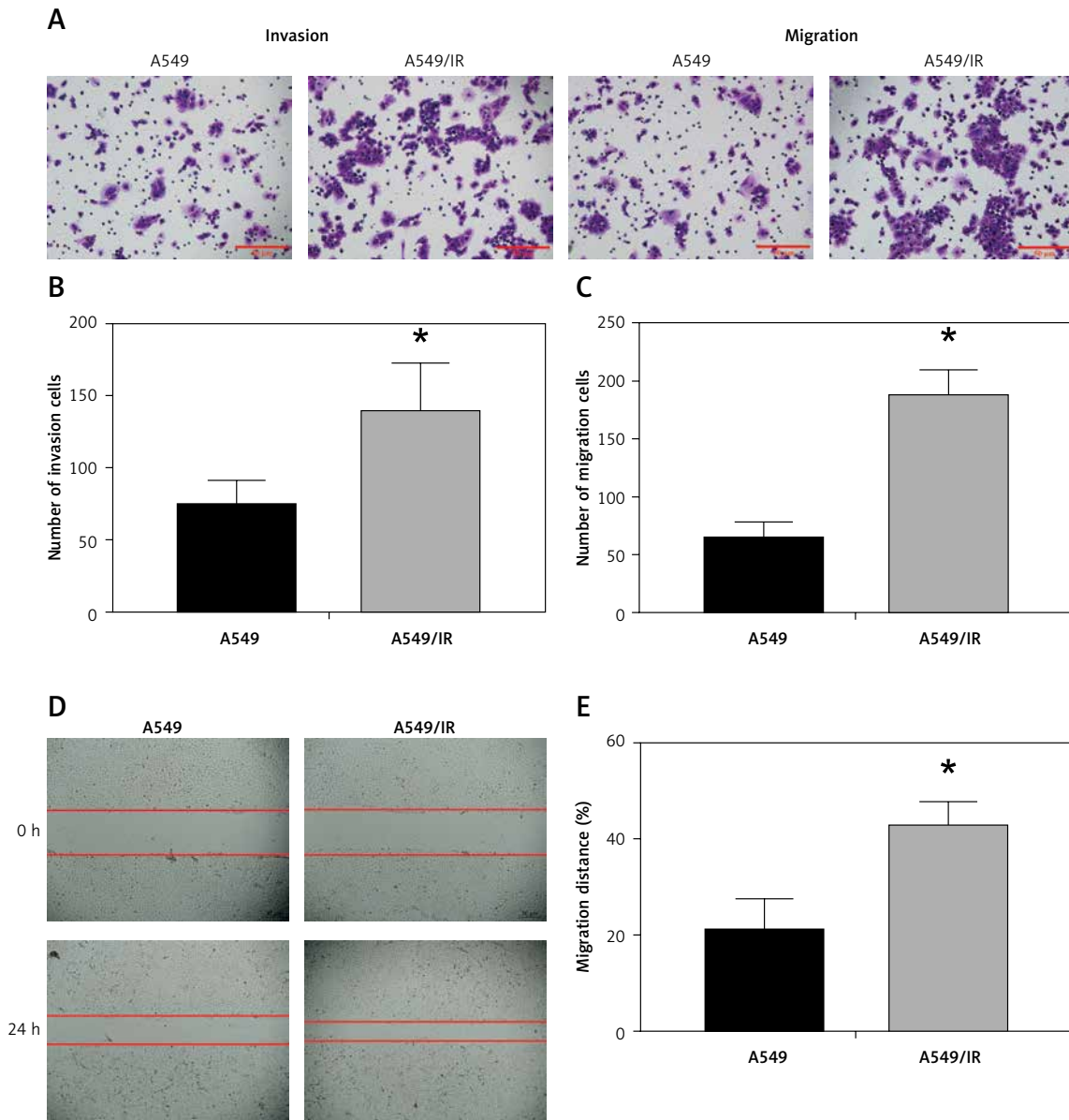


**Figure 2.** Radioresistant non-small-cell lung cancer cells exhibit stronger invasion and migration capabilities. **A–C** – Invasion by the A549 cells after different doses of cell irradiation was analyzed using the Transwell assay. **D, E** – The migration of A549 cells after different doses of cell irradiation was measured using wound healing assay. Each experiment was performed three times and the data are presented as the mean ± standard deviation  
\* $p < 0.05$  compared to A549 cell group.  $N = 10$ .

As shown in Figures 3 A, D, comparing with that in the control group, OMT treatment could significantly inhibit colony formation by A549 cells *in vitro*. CCK-8 assay also revealed that the proliferation of radioresistant A549 cell lines can be suppressed by OMT treatment (Figure 3 B). The apoptosis of A549 cells after irradiation was next quantified. OMT treatment was demonstrated to aggravate the extent of cell apoptosis *in vitro* (Figures 3 C, E). The apoptosis related proteins (Bcl-2, Bax, cleaved caspase-3, pro-caspase-3, cleaved caspase-8, pro-caspase-8, cleaved caspase-9, pro-caspase-9) were measured using western blot (Figure 4). Figures 4 A, B showed that the expression of Bcl-2 was

significantly decreased in the OMT group ( $p < 0.05$ ), while the expression of Bax was significantly increased in the OMT group ( $p < 0.05$ ). Figures 4 C, D showed that the ratios of cleaved caspase-3/pro-caspase-3, cleaved caspase-8/pro-caspase-8, and cleaved caspase-9/pro-caspase-9 were all significantly increased in the OMT group ( $p < 0.05$ ).

#### OMT treatment suppresses irradiation-induced EMT, invasion and migration by NSCLC cells

As radioresistant A549 cells have likely acquired the mesenchymal phenotype, we next investi-

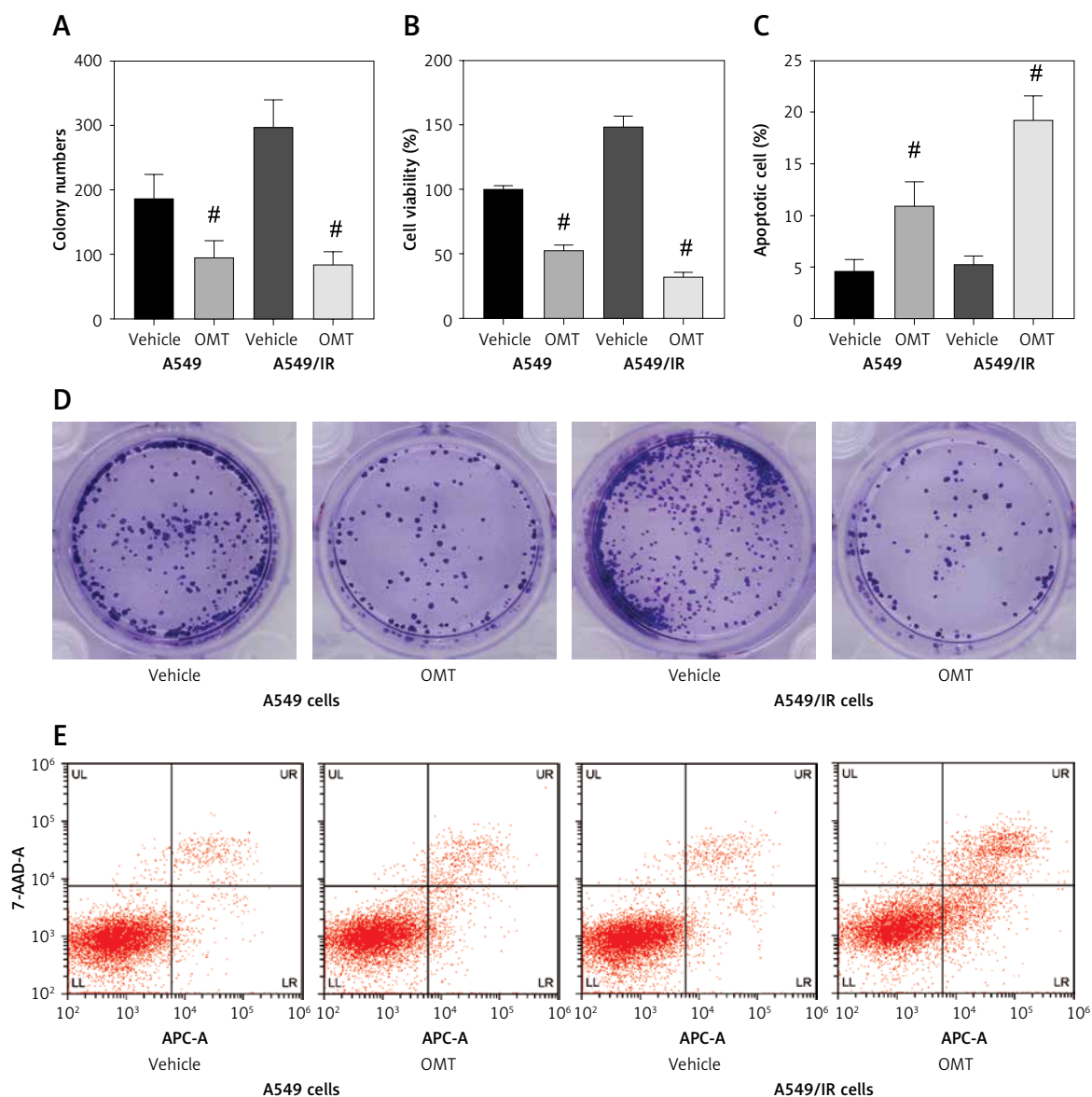


**Figure 3.** Oxymatrine treatment restores the radiosensitivity of non-small-cell lung cancer cells by suppressing colony formation, proliferation and aggravating apoptosis. **A, D** – Colony formation by A549 cells after cell irradiation and OMT treatment was analyzed by colony formation assay. **B** – The viability of A549 cells was analyzed using the Cell Counting Kit-8 assay. **C, E** – The apoptosis of A549 cells after cell irradiation and OMT treatment was analyzed by flow cytometry. Each experiment was performed three times and measured data are presented as the mean  $\pm$  standard deviation

OMT – oxymatrine, # $p < 0.05$  compared to vehicle group.  $N = 10$ .

gated the impact of OMT on irradiation-induced EMT in NSCLC cells. After treatment with OMT, E-cadherin expression was upregulated whereas vimentin expression was downregulated (Figures 5 A–C). These evidences suggest that OMT treatment can suppress irradiation-induced EMT in NSCLC cells. Subsequently, we performed Transwell invasion and wound healing assays to analyze their invasive and migratory capabilities in each A549 cell group. The irradiation-induced invasion and migration by A549 cells was found to be suppressed by OMT treatment (Figures 5 D–F).

### DcR3/AKT/GSK-3 $\beta$ signalling is activated in radioresistant NSCLC cells

A previous clinical study of 365 cases found that DcR3 is associated with the tumorigenesis and deterioration of lung cancer [15]. In addition, AKT/GSK-3 $\beta$  was found to be one of the downstream components of DcR3 [16]. Therefore, we explored the effect of the DcR3/AKT/GSK-3 $\beta$  pathway on the development of radioresistance in NSCLC cells. After cell irradiation, the DcR3/AKT/GSK-3 $\beta$  pathway in A549 cells was markedly activated in a dose-dependent manner (Figures 6 A–C). We

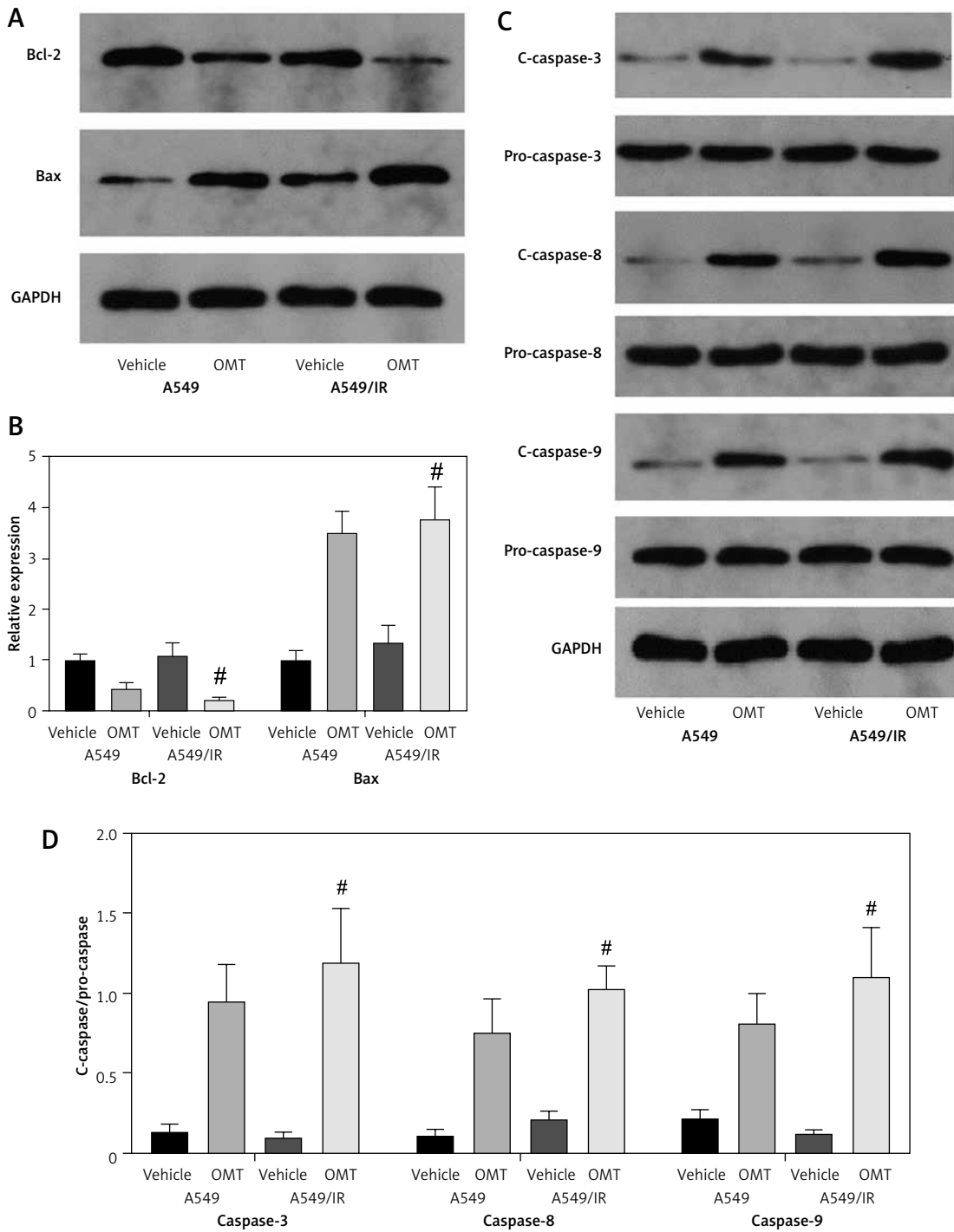


**Figure 4.** Oxymatrine treatment changed the expression of apoptosis-related proteins. **A** – The Representative western blots of Bcl-2 and Bax in A549 cells. **B** – The relative expression of Bcl-2 and Bax in A549 cells. **C** – The representative western blots of Bax, Bcl-2, cleaved caspase-3, pro-caspase-3, cleaved caspase-8, pro-caspase-8, cleaved caspase-9, pro-caspase-9 in A549 cells. **D** – The relative expression of Bax, Bcl-2, cleaved caspase-3, pro-caspase-3, cleaved caspase-8, pro-caspase-8, cleaved caspase-9, pro-caspase-9 in A549 cells. Each experiment was performed three times and measured data are presented as the mean  $\pm$  standard deviation.

OMT – oxymatrine, # $p < 0.05$  compared to vehicle group.  $N = 10$ .



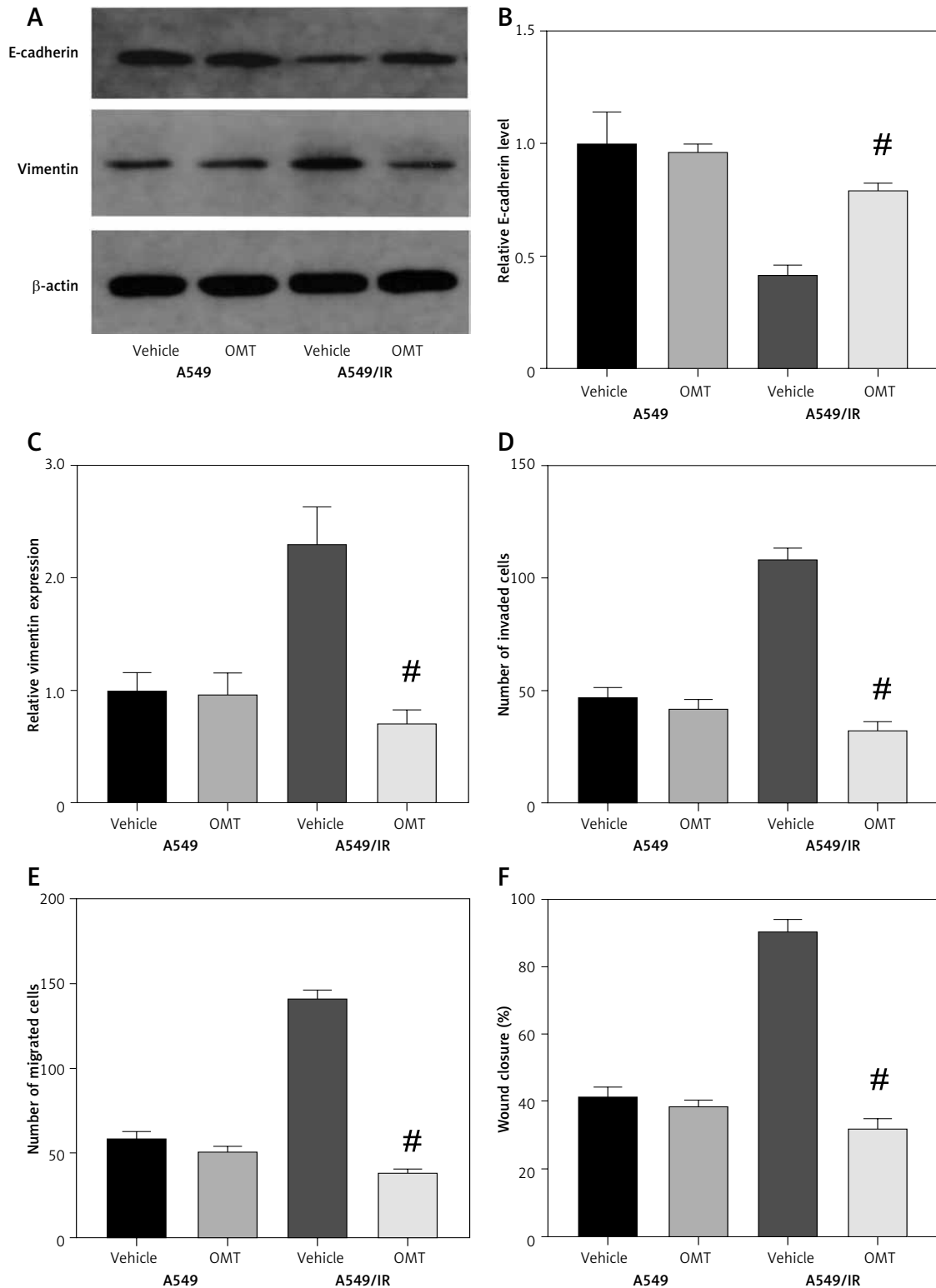


**Figure 5.** Oxymatrine treatment suppresses irradiation-induced EMT, invasion and migration of NSCLC cells. **A–C** – The protein expression of EMT markers E-cadherin and vimentin in A549 cells after cell irradiation and OMT treatment.  $\beta$ -actin was used for normalization. **D, E** – The degree of invasion by A549 cells after cell irradiation and OMT treatment was analyzed using the Transwell invasion assay. **F** – The migration of A549 cells after cell irradiation and OMT treatment was analyzed using wound healing assay. Each experiment was performed three times and the data are presented as the mean  $\pm$  standard deviation

OMT – oxymatrine, EMT – epithelial-mesenchymal transition, # $p < 0.05$  compared to vehicle group.  $N = 10$ .

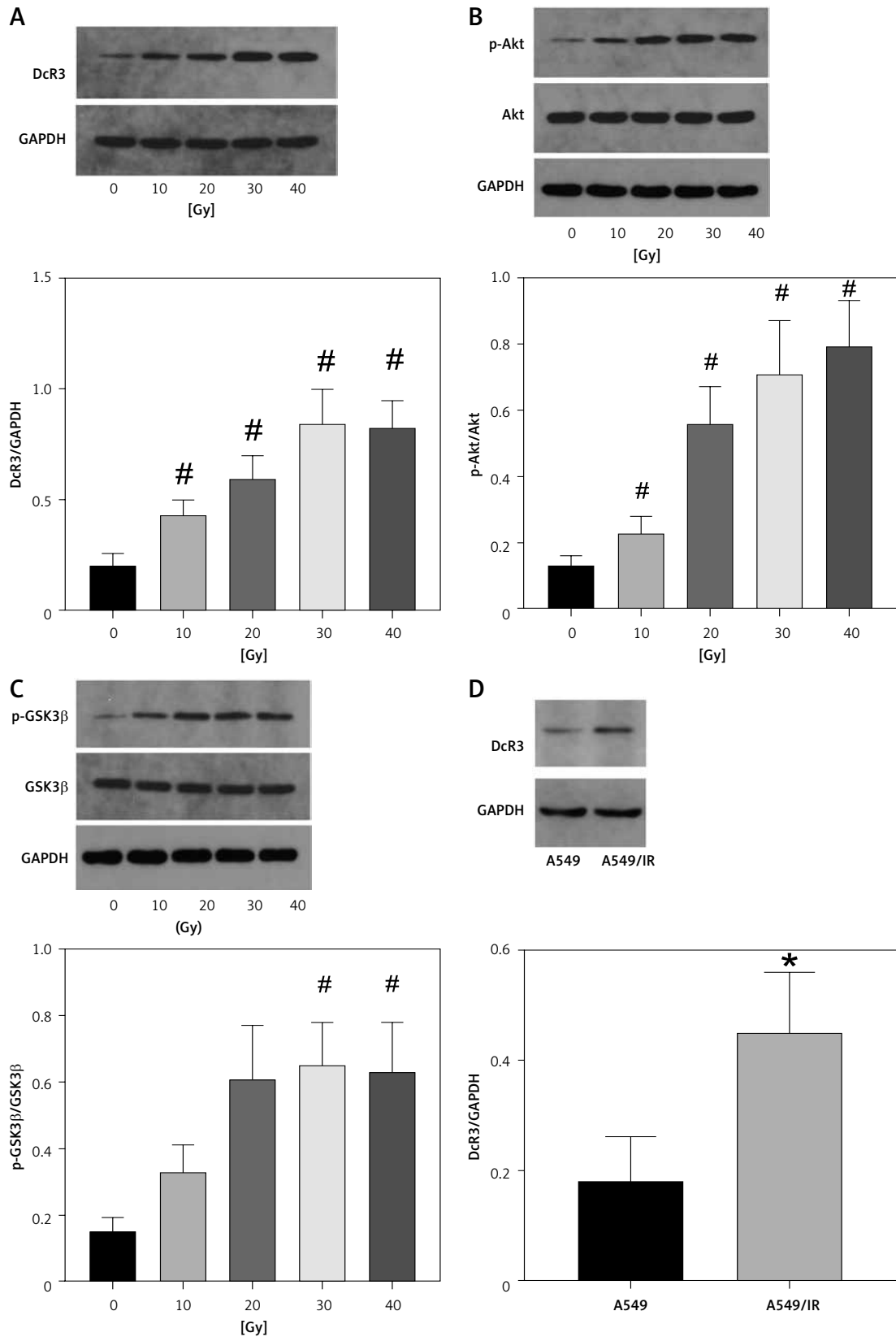


**Figure 6.** DcR3/AKT/GSK-3 $\beta$  signaling is activated in radioresistant non-small-cell lung cancer cells. **A–C** – Activity of the DcR3/AKT/GSK-3 $\beta$  pathway after different doses of cell irradiation.  $\beta$ -actin was used for normalization. **D–F** – Activity of the DcR3/AKT/GSK-3 $\beta$  pathway after cell irradiation.  $\beta$ -actin was used for normalization. Each experiment was performed three times and the measured data are presented as the mean  $\pm$  standard deviation. DcR3 – decoy receptor 3, AKT – protein kinase B, GSK-3 – glycogen synthase kinase-3 $\beta$ , \* $p < 0.05$  compared to A549 cell group, # $p < 0.05$  compared to 0 Gy group.  $N = 10$ .

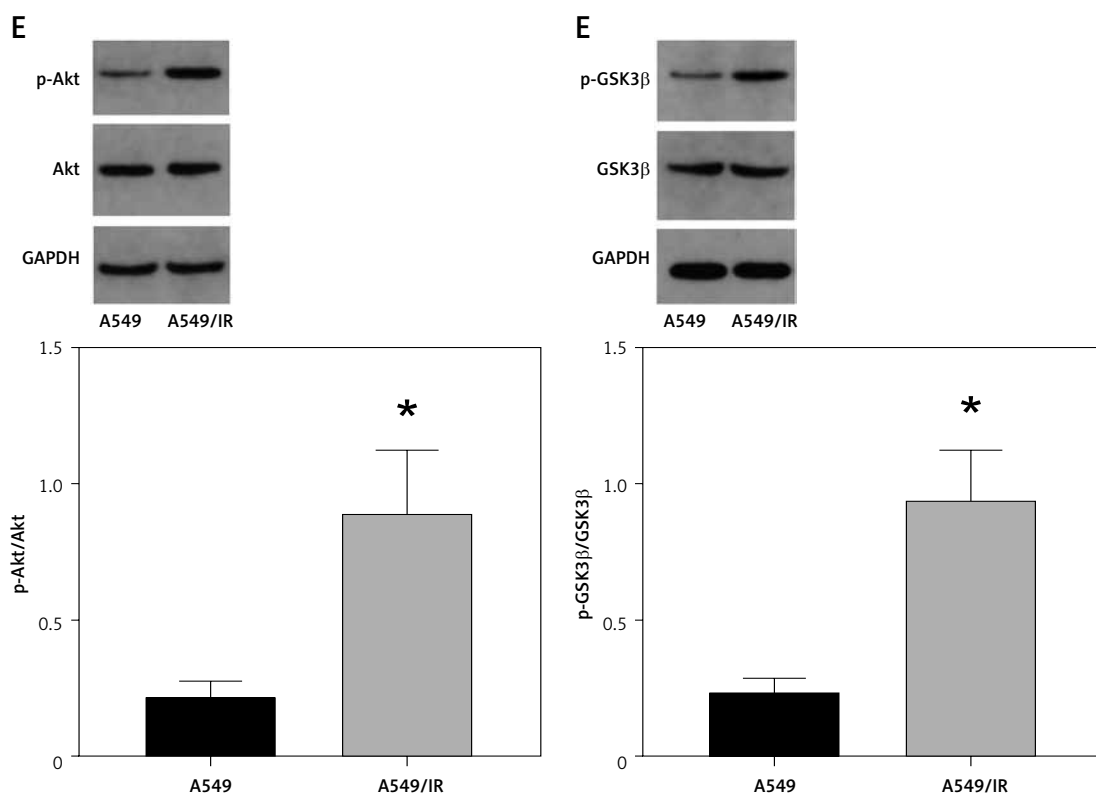


**Figure 6.** Cont. E–F – Activity of the DcR3/AKT/GSK-3 $\beta$  pathway after cell irradiation.  $\beta$ -actin was used for normalization. Each experiment was performed three times and the measured data are presented as the mean  $\pm$  standard deviation

DcR3 – decoy receptor 3, AKT – protein kinase B, GSK-3 – glycogen synthase kinase-3 $\beta$ , \* $p < 0.05$  compared to A549 cell group, # $p < 0.05$  compared to 0 Gy group. N = 10.

then measured the activity of DcR3/AKT/GSK-3 $\beta$  signaling in radioresistant A549 cells, which was found to be significantly activated in radioresistant A549 cells (Figures 6 D–F).

#### OMT treatment restores radiosensitivity in NSCLC cells and inhibits irradiation-induced EMT, invasion and migration through the DcR3/AKT/GSK-3 $\beta$ pathway

Subsequently, we analyzed the effects of OMT on irradiated NSCLC cells with focus on the DcR3/AKT/GSK-3 $\beta$  axis *in vitro*. As shown in Figures 7 A–C, activation of the DcR3/AKT/GSK-3 $\beta$  axis was revealed to be significantly inhibited in radioresistant A549 cells after treatment with OMT. These findings suggest that OMT treatment can suppress the activation of DcR3/AKT/GSK-3 $\beta$  signaling in radioresistant NSCLC cells. To explore the role of the DcR3/AKT/GSK-3 $\beta$  pathway in radioresistant NSCLC cells, we treated radioresistant A549 cells with the specific siRNA (DcR3 siRNA, Akt siRNA, or GSK-3 $\beta$  siRNA), then measured the detected the changes of viability, apoptosis, colony formation, invasion, migration, and the protein expression of EMT markers E-cadherin and vimentin in A549 cells (Figure 8). As

shown in Figures 8 A–F, the viability, colony formation, invasion and migration ability of radioresistant A549 cells were all significantly decreased by DcR3 siRNA, Akt siRNA, or GSK-3 $\beta$  siRNA, while the apoptosis rate was significantly decreased by them. As shown in Figures 8 G–I, the E-cadherin expression was upregulated whereas vimentin expression was downregulated by DcR3 siRNA, Akt siRNA, or GSK-3 $\beta$  siRNA in radioresistant A549 cells. To explore the role of the DcR3/AKT/GSK-3 $\beta$  pathway in radioresistant NSCLC cells after OMT treatment further, a number of functional assays were performed on the radioresistant A549 cells. Comparing with that in the untreated control groups, the cell viability of radioresistant A549 cells was decreased after treatment with OMT or the AKT inhibitor MK-2206 (Figure 9 A). In addition, after treatment with OMT and MK-2206, the inhibitory effect did not show significantly differ compared with either treatment alone. These results were also verified by those from colony formation assay, apoptosis, Transwell and wound healing assays, suggesting that OMT treatment can restore radiosensitivity whilst inhibiting irradiation-induced invasion and migration of NSCLC cells, through the AKT pathway (Figures 9 B–F). After treatment with OMT or MK-2206, E-cad-

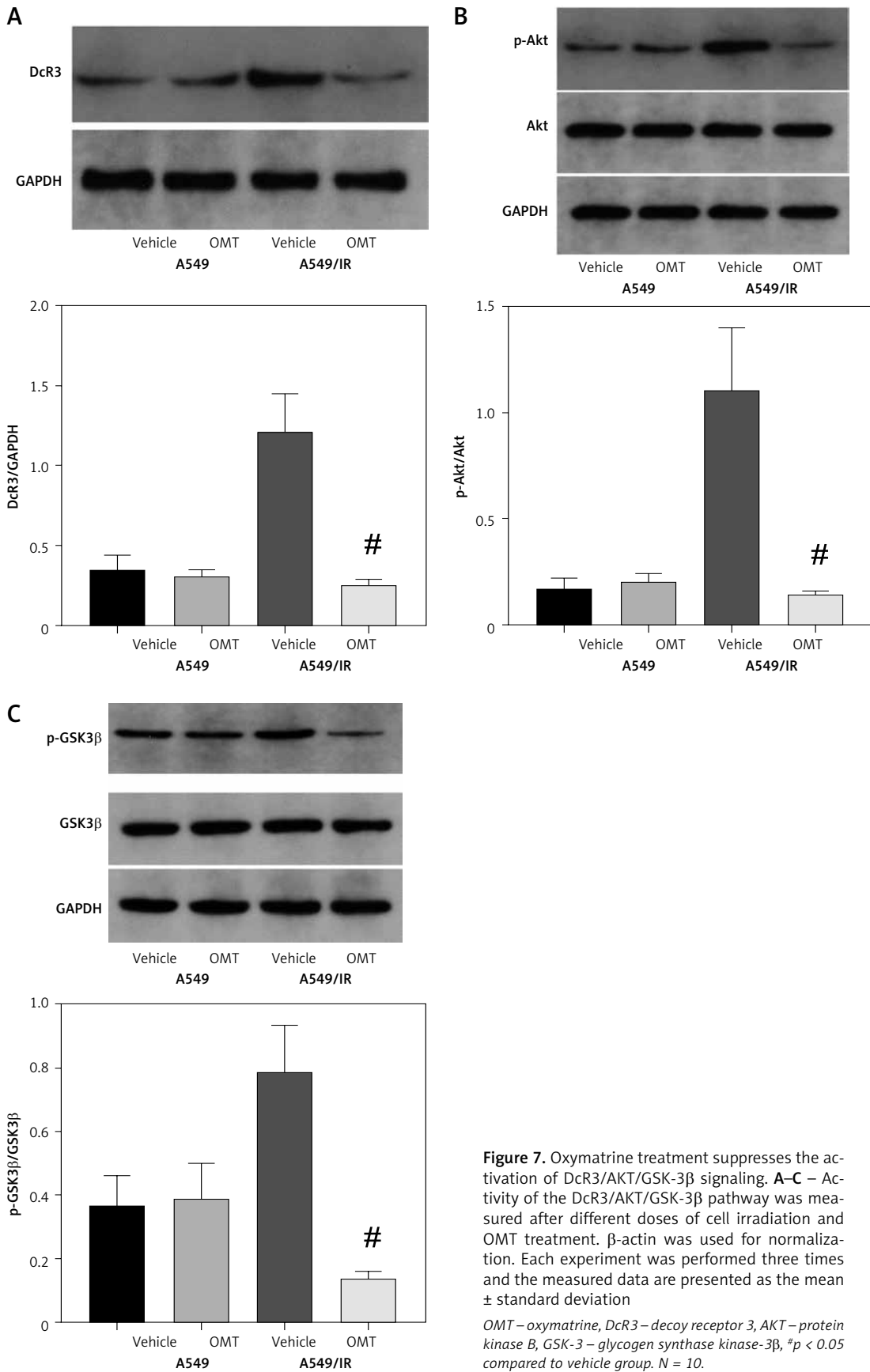


**Figure 7.** Oxymatrine treatment suppresses the activation of DcR3/AKT/GSK-3β signaling. **A–C** – Activity of the DcR3/AKT/GSK-3β pathway was measured after different doses of cell irradiation and OMT treatment. β-actin was used for normalization. Each experiment was performed three times and the measured data are presented as the mean ± standard deviation

OMT – oxymatrine, DcR3 – decoy receptor 3, AKT – protein kinase B, GSK-3 – glycogen synthase kinase-3β, <sup>#</sup>*p* < 0.05 compared to vehicle group. *N* = 10.

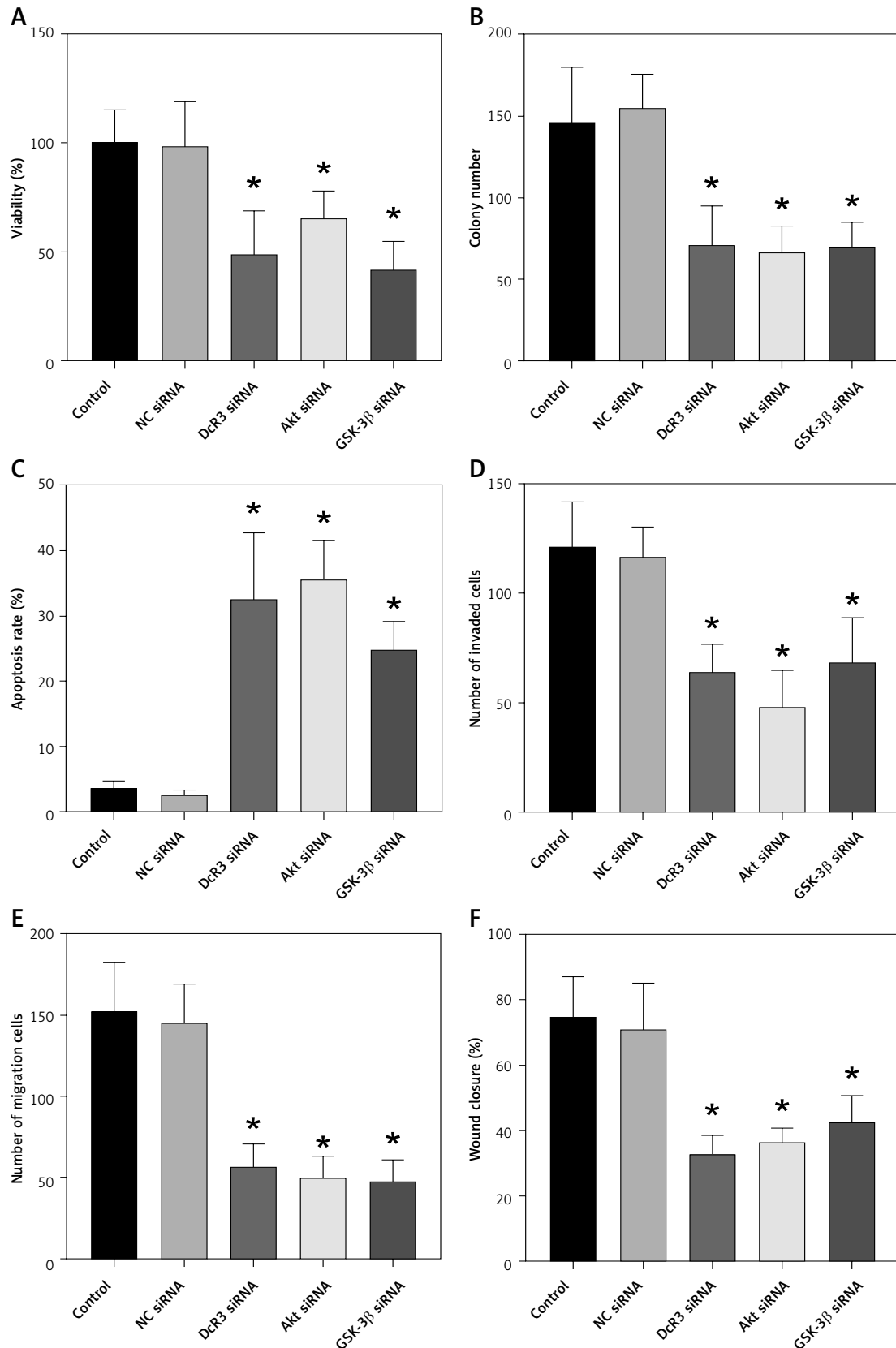


**Figure 8.** The knockdown of DcR3/AKT/GSK-3 $\beta$  changed the viability, apoptosis, colony formation, invasion, migration and EMT in radioresistant A549 cells. **A** – The viability of A549 cells was measured using Cell Counting Kit-8 assay. **B** – Colony formation in A549 cells. **C** – Apoptosis of the A549 cells assessed using flow cytometry. **D** – Invasion by A549 cells analyzed using Transwell invasion assay. **E, F** – The migration of A549 cells measured using transwell migration assay and wound healing assay

DcR3 – decoy receptor 3, AKT – protein kinase B, GSK-3 – glycogen synthase kinase-3 $\beta$ , EMT – epithelial-mesenchymal transition, \* $p < 0.05$  compared to vehicle group.  $N = 10$ .

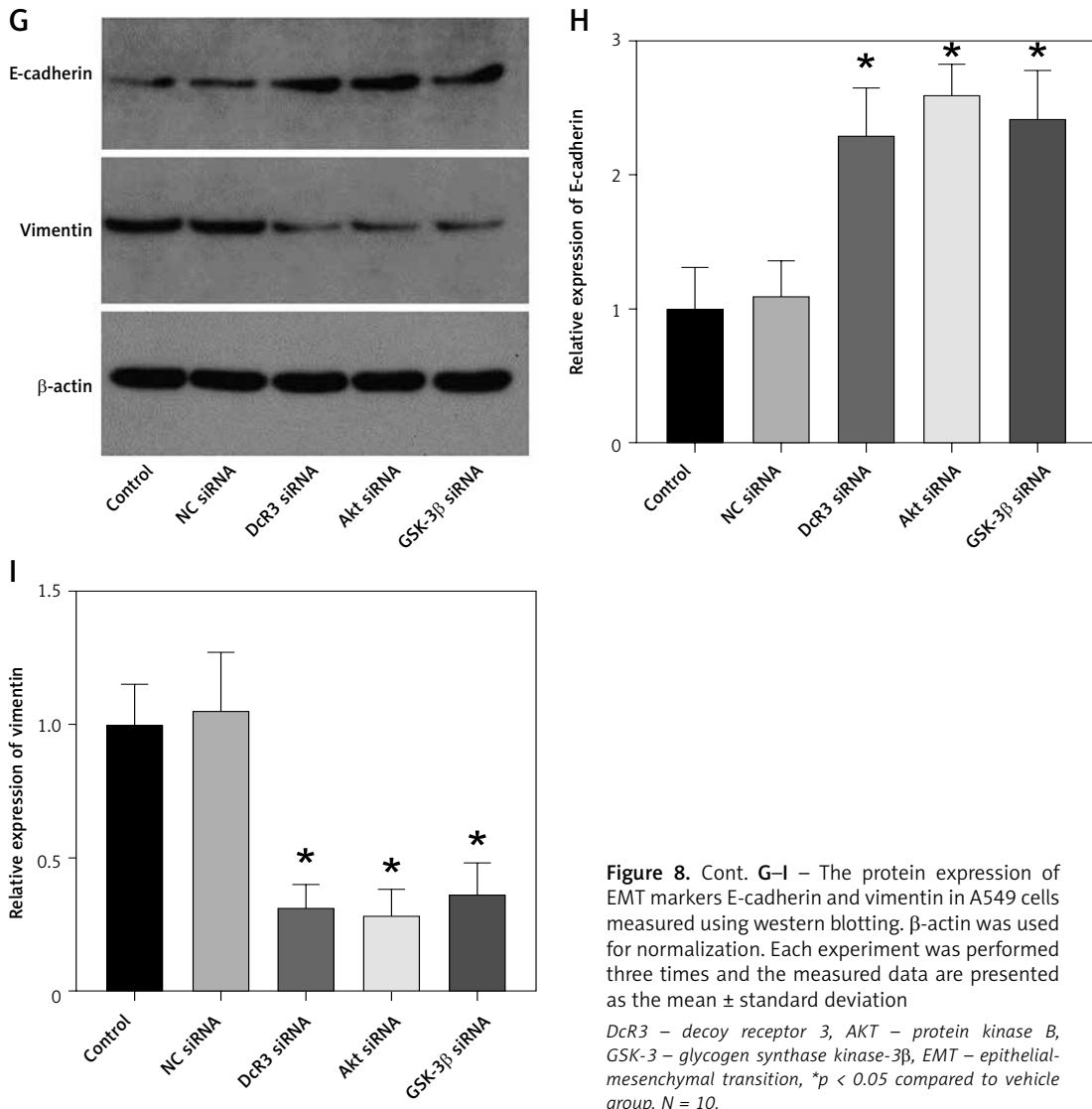


**Figure 8.** Cont. G–I – The protein expression of EMT markers E-cadherin and vimentin in A549 cells measured using western blotting.  $\beta$ -actin was used for normalization. Each experiment was performed three times and the measured data are presented as the mean  $\pm$  standard deviation

DcR3 – decoy receptor 3, AKT – protein kinase B, GSK-3 – glycogen synthase kinase-3 $\beta$ , EMT – epithelial-mesenchymal transition, \* $p < 0.05$  compared to vehicle group.  $N = 10$ .

herin expression was upregulated whereas vimentin expression was downregulated in radioresistant A549 cells (Figures 9 G–I). These results suggest that OMT treatment can inhibit irradiation-induced EMT in NSCLC cells through AKT.

**OMT treatment restores radiosensitivity and inhibits irradiation-induced EMT, invasion and migration in NSCLC cells through the DcR3/AKT/GSK-3 $\beta$  pathway**

We next assessed if OMT treatment mediates its function in irradiated NSCLC cells through the DcR3/AKT/GSK-3 $\beta$  pathway *in vitro*. Firstly, we successfully overexpressed DcR3 in A549 cells and before cell irradiation was performed to establish the radioresistant phenotype (Figure 10 A). We then quantified the expression of AKT and GSK-3 $\beta$  in each treatment group of A549 cells. Overexpression of DcR3 was able to activate AKT/GSK-3 $\beta$  signaling *in vitro* (Figure 10 B, C). By contrast, OMT

treatment could reverse the activation of the AKT/GSK-3 $\beta$  pathway in irradiated A549 cells.

Results from functional assays, including those from apoptosis (Figure 10 D), Transwell invasion (Figures 10 E, F), wound healing (Figure 10 G) and proliferation assays (Figure 10 H), also supported the results aforementioned. After overexpressing DcR3, the apoptosis of radioresistant A549 cells was inhibited, whereas the invasion, migration and proliferation of radioresistant A549 cells was promoted. however, OMT treatment could restore the functional influence of DcR3 overexpression in radioresistant A549 cells, which may restore the radiosensitivity of A549 cells.

**OMT treatment promotes the inhibitory effects of radiation on tumor growth in radioresistant xenograft models**

We subsequently explored if OMT treatment can also restore radiosensitivity in NSCLC *in vivo*.

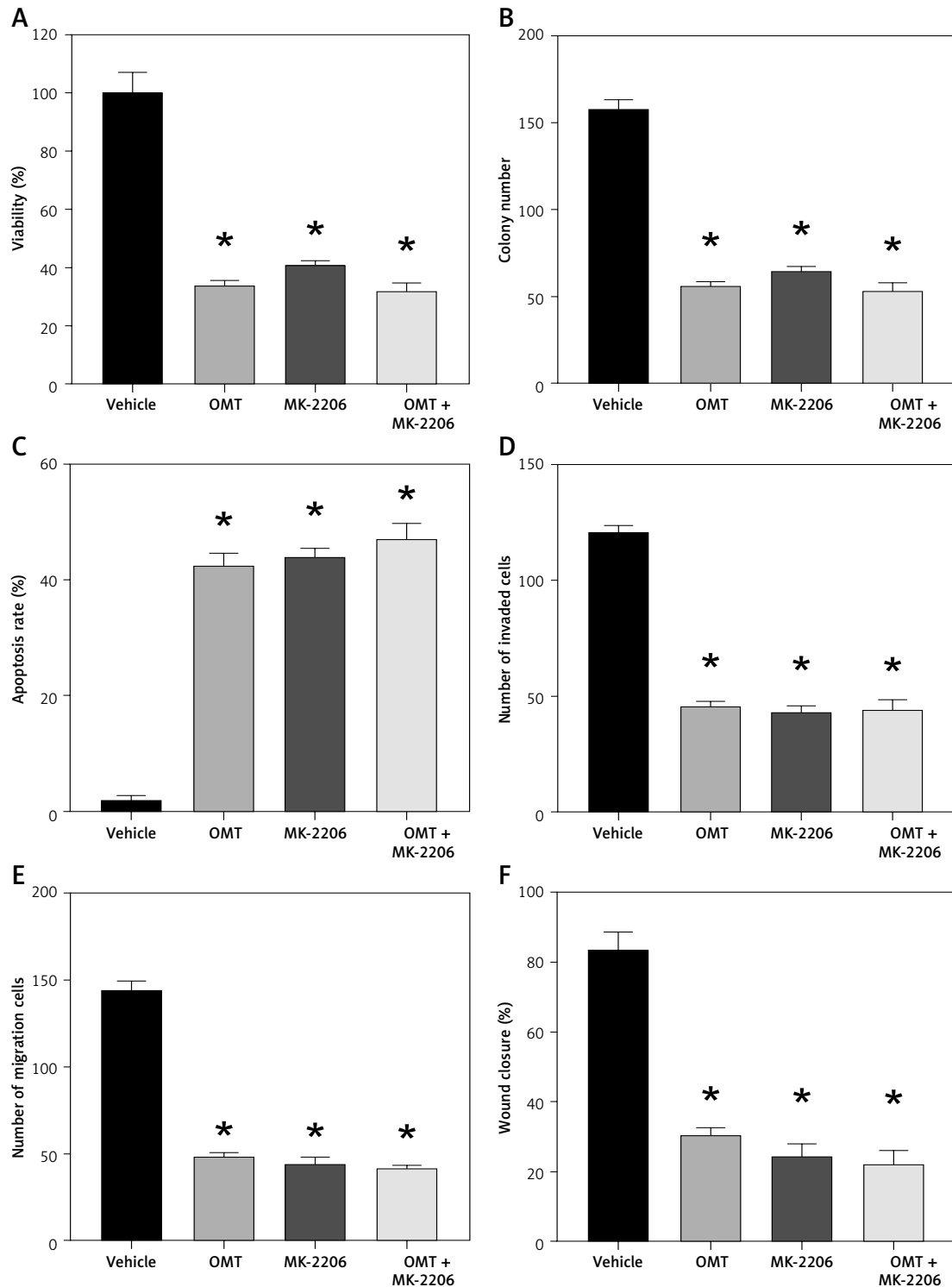


**Figure 9.** Oxymatrine treatment restores radiosensitivity in non-small-cell lung cancer cells to inhibit EMT, invasion and migration through the DcR3/AKT/GSK-3 $\beta$  pathway. **A** – The viability of A549 cells was measured after cell irradiation, OMT and MK-2206 treatment using Cell Counting Kit-8 assay. **B** – Colony formation by A549 cells was measured after cell irradiation, OMT and MK-2206 treatment. **C** – Apoptosis of the A549 cells after cell irradiation, OMT and MK-2206 treatment was assessed using flow cytometry. **D** – Invasion by A549 cells after cell irradiation, OMT and MK-2206 treatment was analyzed using Transwell invasion assay. **E, F** – The migration of A549 cells after cell irradiation, OMT and MK-2206 treatment was measured using Transwell migration assay and wound healing assay. OMT – oxymatrine, DcR3 – decoy receptor 3, AKT – protein kinase B, GSK-3 – glycogen synthase kinase-3 $\beta$ , EMT – epithelial-mesenchymal transition, \* $p < 0.05$  compared to vehicle group,  $N = 10$ .

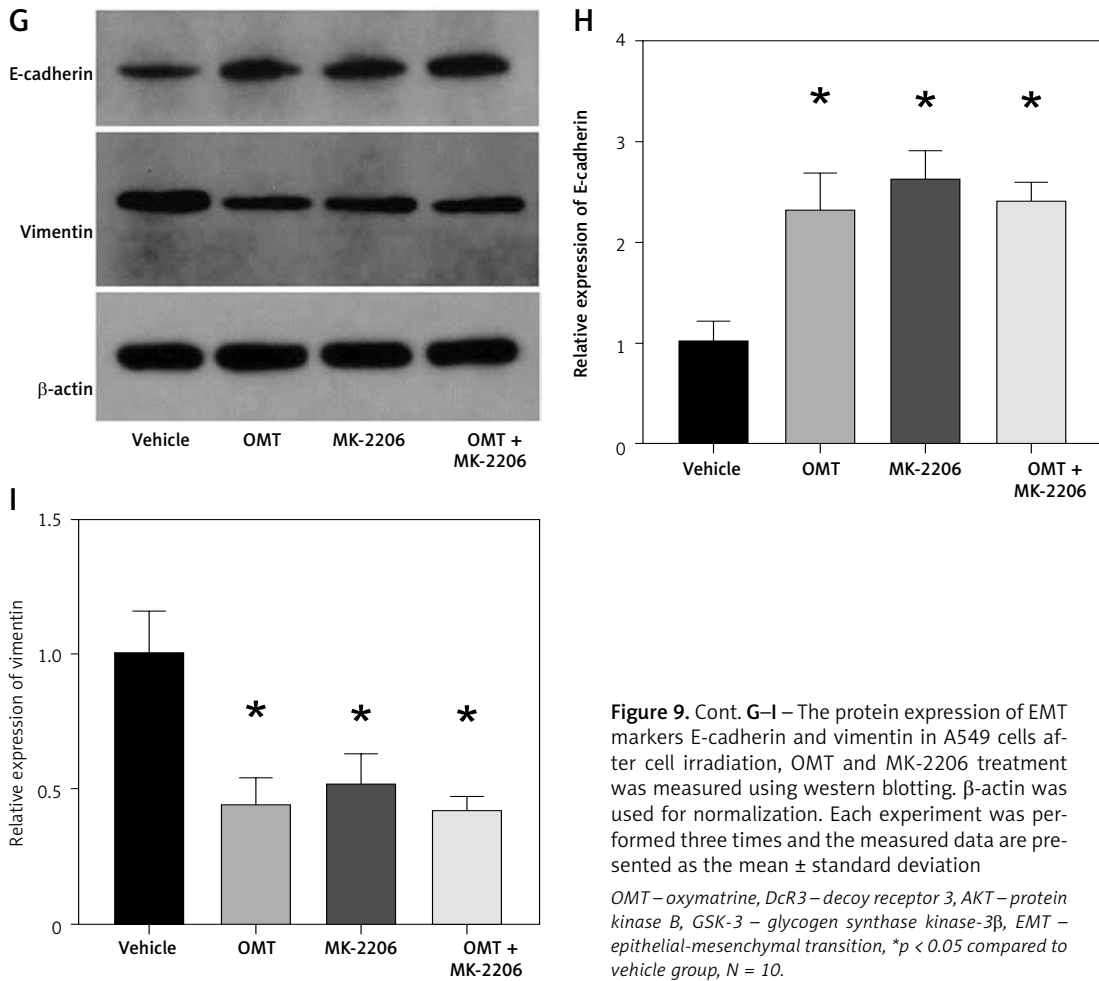


**Figure 9.** Cont. G–I – The protein expression of EMT markers E-cadherin and vimentin in A549 cells after cell irradiation, OMT and MK-2206 treatment was measured using western blotting.  $\beta$ -actin was used for normalization. Each experiment was performed three times and the measured data are presented as the mean  $\pm$  standard deviation  
 OMT – oxymatrine, DcR3 – decoy receptor 3, AKT – protein kinase B, GSK-3 – glycogen synthase kinase-3 $\beta$ , EMT – epithelial-mesenchymal transition, \* $p < 0.05$  compared to vehicle group,  $N = 10$ .

As shown in Figures 11 A–C, after treatment with OMT, the xenograft tumor size and weight from mice that underwent radiotherapy were decreased *in vivo*. We next counted the number of metastatic nodules in the mice body and found that OMT treatment could also inhibit tumor metastasis in the xenograft tumor models (Figure 11 D).

We next measured the extent of irradiation-induced EMT and activation of the DcR3/AKT/GSK-3 $\beta$  pathway in the xenograft tumor models. DcR3 expression was found to be downregulated in OMT-treated animals (Figure 12 A). Additionally, after treatment with OMT, E-cadherin expression was increased whilst vimentin expression was decreased, suggesting that OMT treatment inhibited irradiation-induced EMT *in vivo* (Figures 12 B, C). We also found that DcR3/AKT/GSK-3 $\beta$  signaling was activated in the radioresistant xenograft tumor models (Figures 12 D–F).

**Discussion**

Non-small cell lung cancer is a prevalent malignancy and a leading cause of cancer-associated mortality worldwide, which accounts for 80-85%

all lung cancer cases [17]. Similar to the therapeutic strategy of other malignancies, radiotherapy serves a key role in NSCLC clinical treatment. However, radioresistance poses a major obstacle to the efficacy of radiotherapy for NSCLC. Although studies previously reporting the molecular mechanism underlying radioresistance in NSCLC have been performed, the specific mechanism remains unclear. Therefore, deepening the understanding into the mechanism of radioresistant and exploration of novel therapeutic strategies to restore radiosensitivity may prove effective for NSCLC treatment [18]. In this study, we explored the impact of OMT in NSCLC radioresistance. Our analysis revealed that the DcR3/AKT/GSK-3 $\beta$  pathway was activated in radioresistant NSCLC cells. Subsequent functional experiments also demonstrated that OMT treatment can restore radiosensitivity in NSCLC cells to in turn inhibit colony formation and proliferation whilst promoting cell apoptosis. To the best of our knowledge, the study was the first that reported the potentially restorative effects of OMT on the radiosensitivity of NSCLC.

Oxymatrine was chosen study in this study as a result of previous reports documenting its



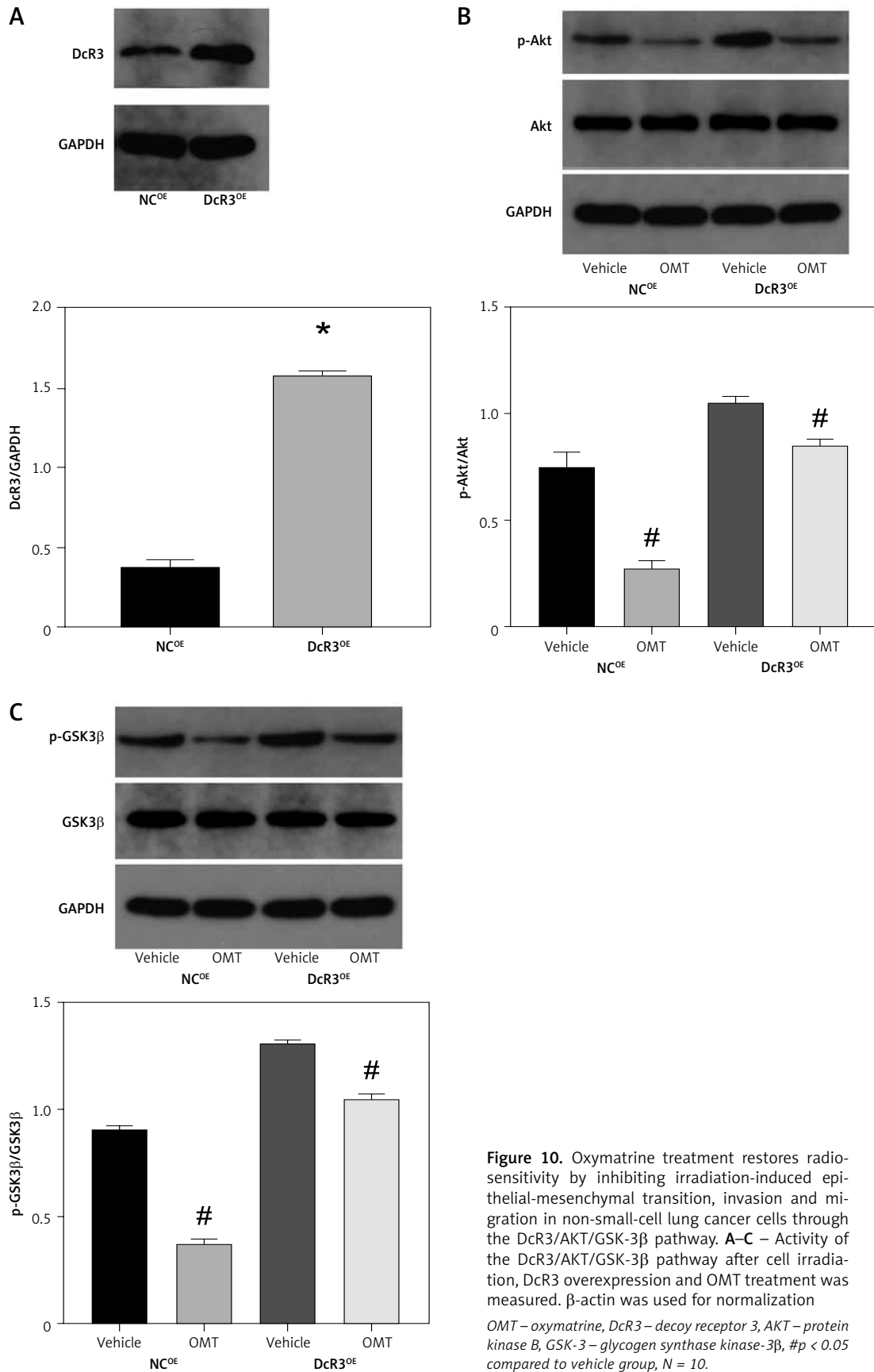


**Figure 10.** Oxymatrine treatment restores radio-sensitivity by inhibiting irradiation-induced epithelial-mesenchymal transition, invasion and migration in non-small-cell lung cancer cells through the DcR3/AKT/GSK-3 $\beta$  pathway. **A–C** – Activity of the DcR3/AKT/GSK-3 $\beta$  pathway after cell irradiation, DcR3 overexpression and OMT treatment was measured.  $\beta$ -actin was used for normalization  
OMT – oxymatrine, DcR3 – decoy receptor 3, AKT – protein kinase B, GSK-3 – glycogen synthase kinase-3 $\beta$ , # $p < 0.05$  compared to vehicle group,  $N = 10$ .

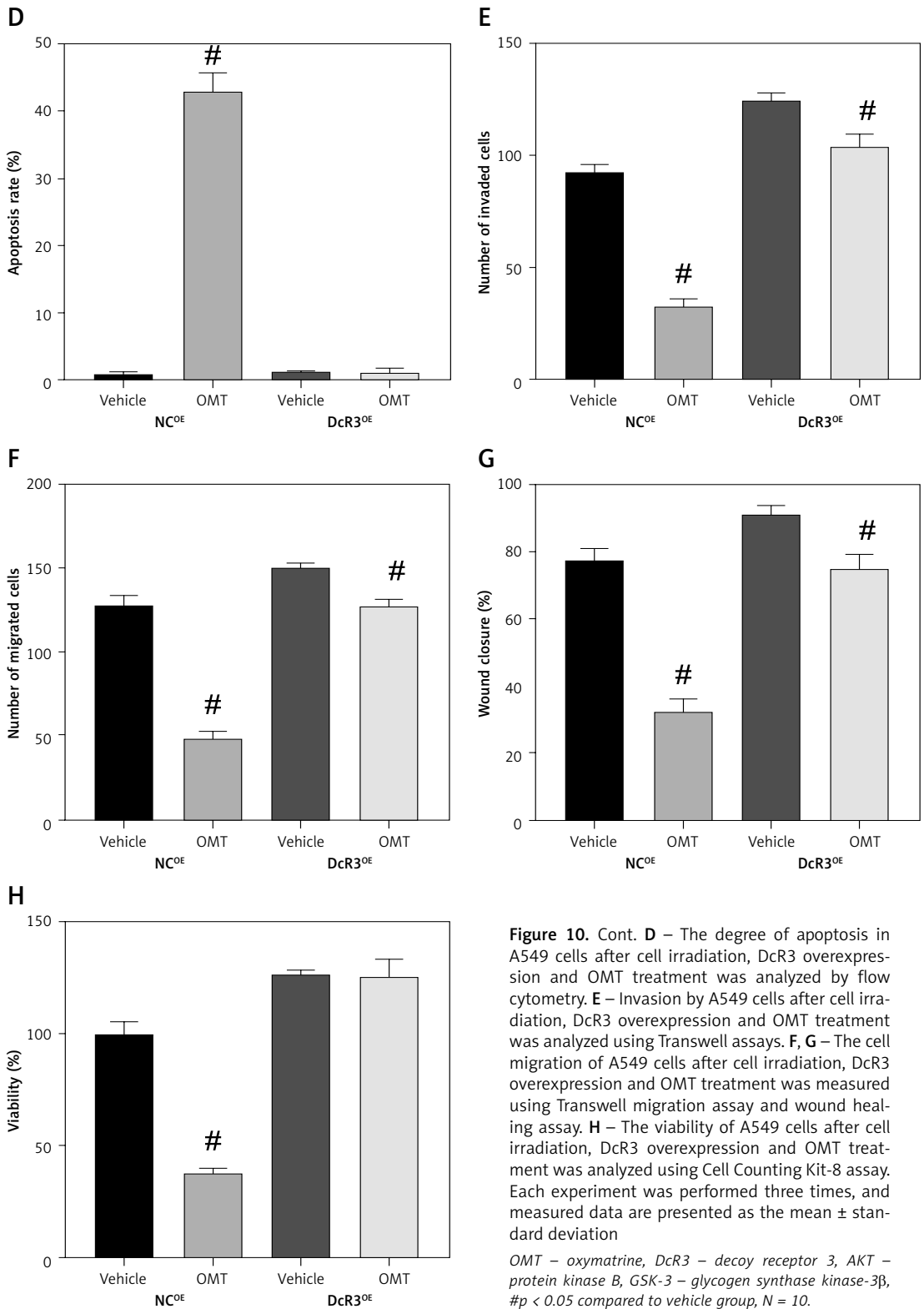


**Figure 10.** Cont. **D** – The degree of apoptosis in A549 cells after cell irradiation, DcR3 overexpression and OMT treatment was analyzed by flow cytometry. **E** – Invasion by A549 cells after cell irradiation, DcR3 overexpression and OMT treatment was analyzed using Transwell assays. **F, G** – The cell migration of A549 cells after cell irradiation, DcR3 overexpression and OMT treatment was measured using Transwell migration assay and wound healing assay. **H** – The viability of A549 cells after cell irradiation, DcR3 overexpression and OMT treatment was analyzed using Cell Counting Kit-8 assay. Each experiment was performed three times, and measured data are presented as the mean ± standard deviation

OMT – oxymatrine, DcR3 – decoy receptor 3, AKT – protein kinase B, GSK-3 – glycogen synthase kinase-3 $\beta$ , #*p* < 0.05 compared to vehicle group, N = 10.

protective effects on NSCLC progression [5, 6]. Furthermore, OMT has been reported to exert anti-oxidation, anti-inflammation and anti-apoptotic properties, leading to therapeutic effects against many diseases, including heart failure, influenza a virus and diabetic [19–21]. Since the potential

the potential effects of OMT and NSCLC remain unknown, this study reported for the first time that OMT can restore radiosensitivity in NSCLC cells to reverse irradiation-induced EMT, inhibit invasion and migration by targeting the DcR3/ AKT/GSK-3 $\beta$  pathway. We also found that OMT

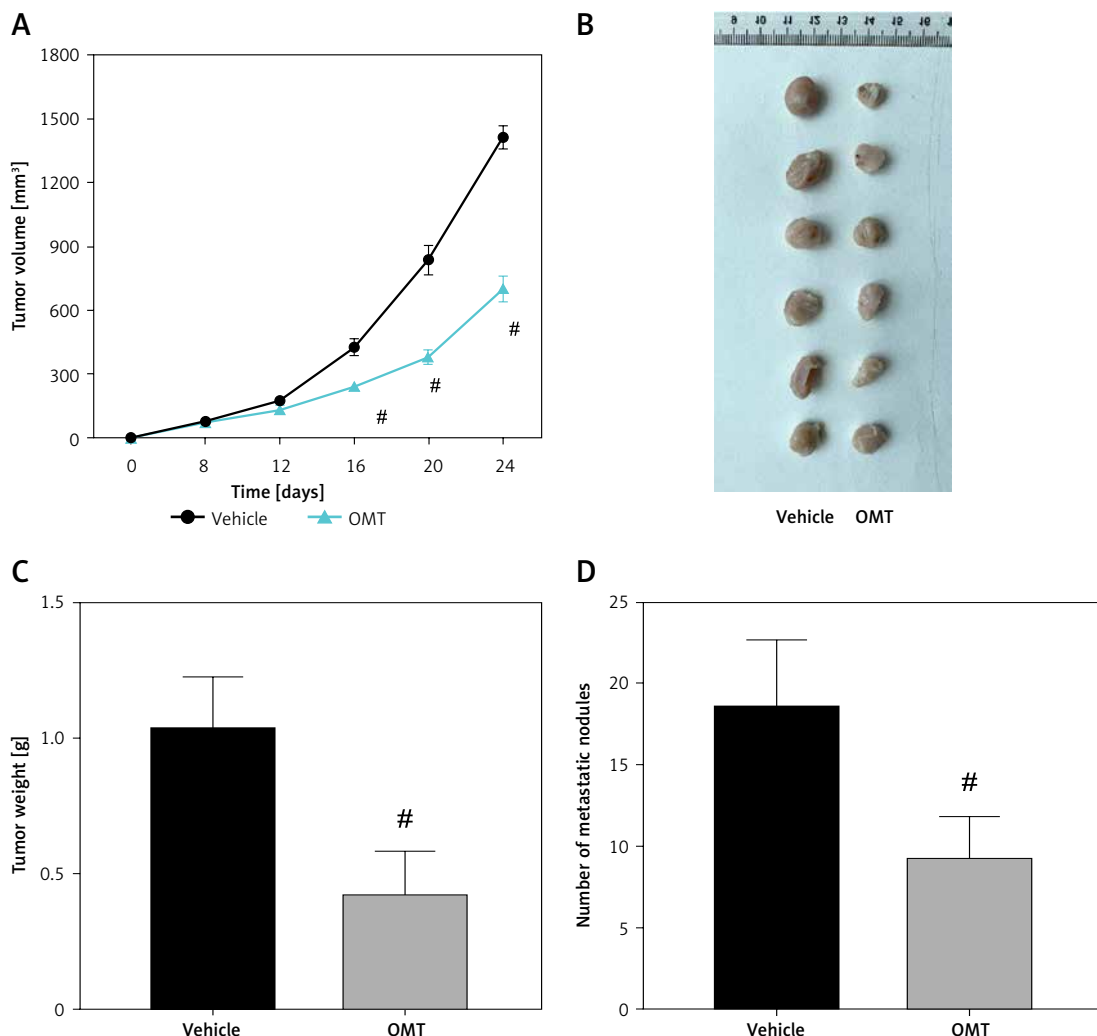


**Figure 11.** Oxymatrine treatment inhibits tumor growth in radioresistant xenograft tumors. **A–C** – The volume and weight of the xenograft tumors after treatment with OMT and radiotherapy. **D** – The metastatic nodules of the xenograft tumors after treatment with OMT and radiotherapy. Each experiment was performed three times and the measured data are presented as the mean  $\pm$  standard deviation

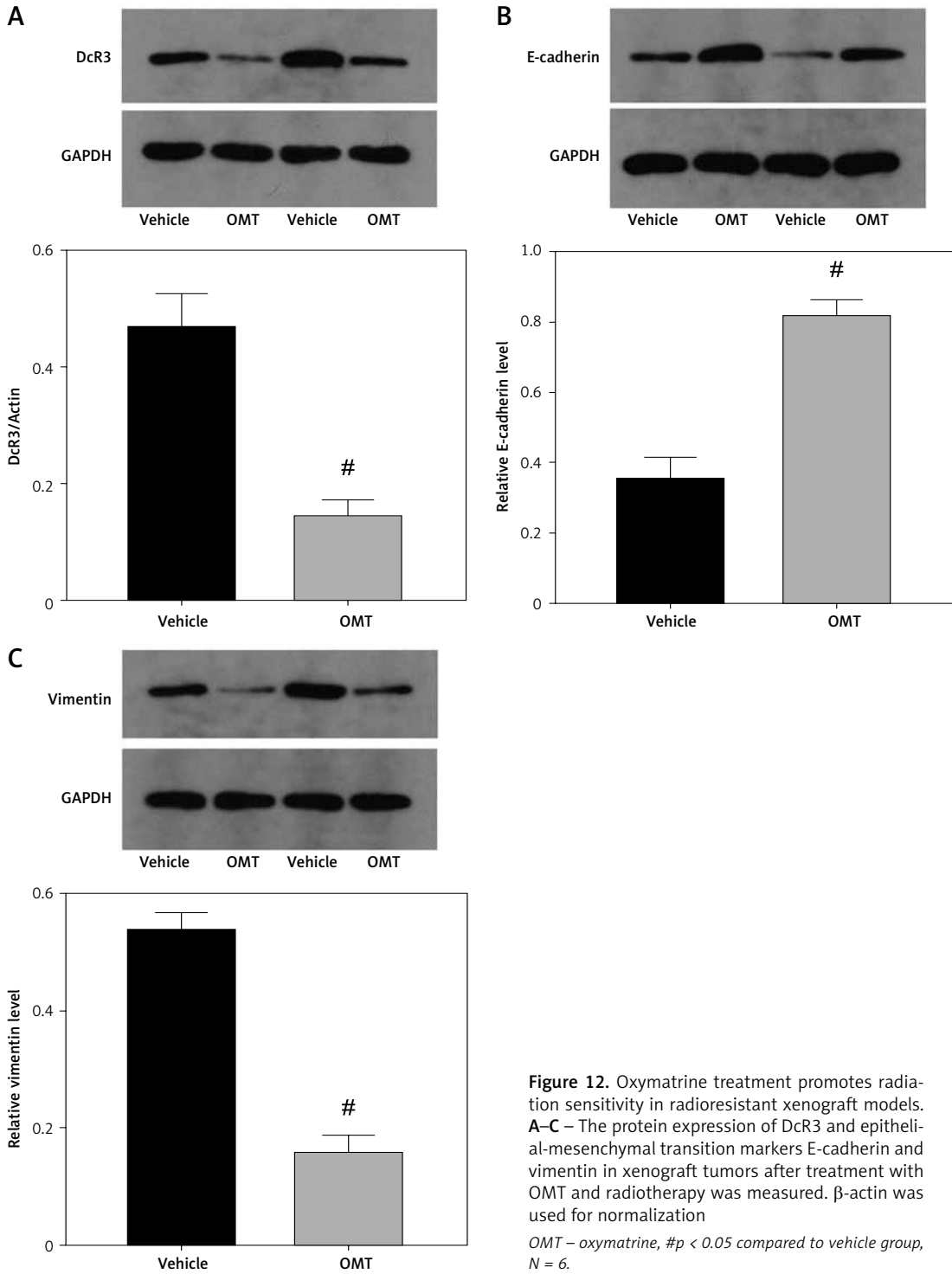
OMT – oxymatrine, #  $p < 0.05$  compared to vehicle group,  $N = 6$ .

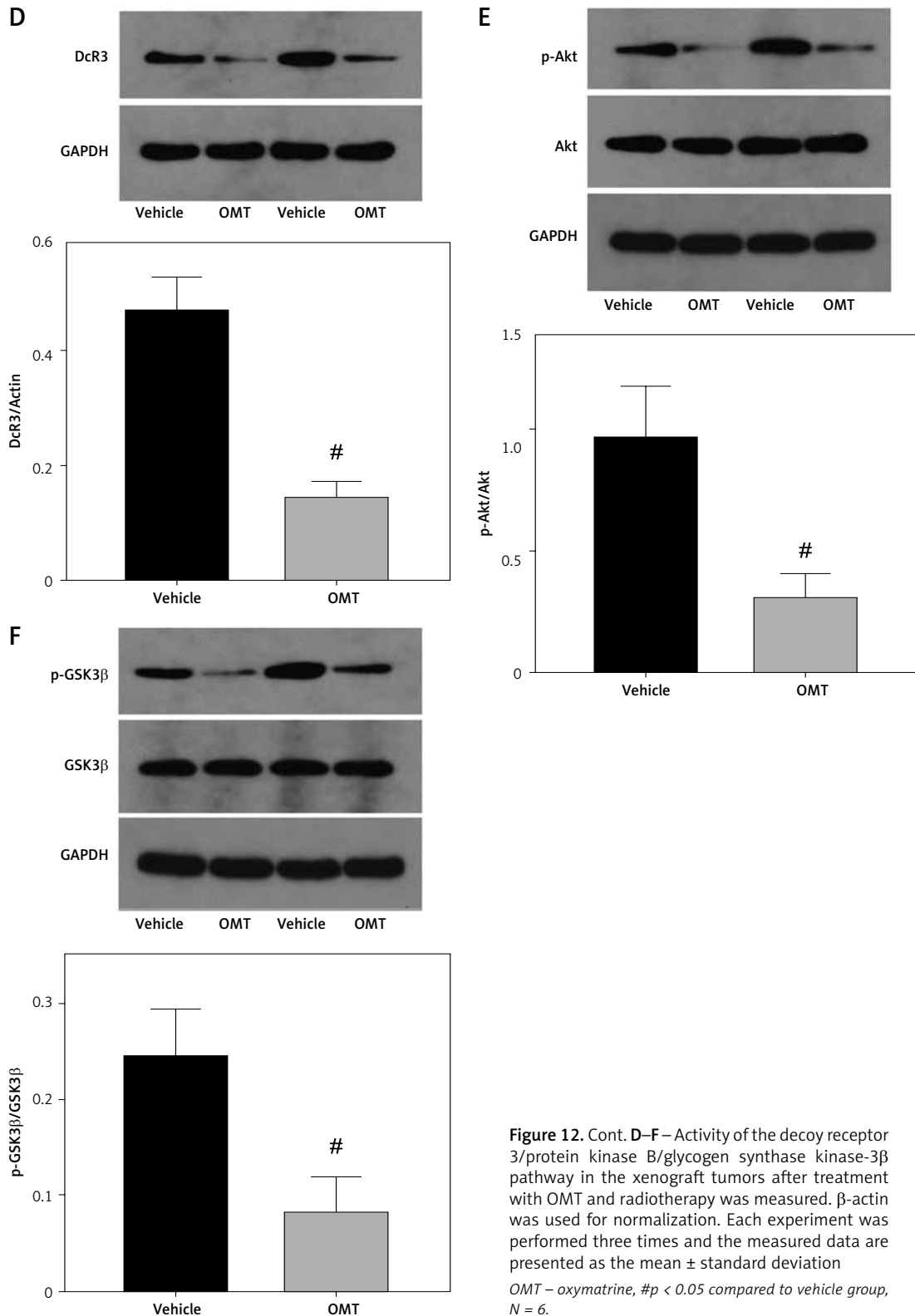
treatment was able to suppress colony formation, proliferation whilst aggravating the apoptosis of A549 cells *in vitro*. In addition, OMT treatment promoted the inhibitory effects of radiation on tumor growth in radioresistant xenograft tumors. In summary, these findings suggest that OMT hold potential for use in combination with NSCLC radiotherapy in a clinical setting.

Tumor metastasis and recurrence are the main causes of the high mortality rate of NSCLC, where EMT serves an important role in initiation of cancer metastasis [22]. During the progression of EMT, cancer cells of the epithelial phenotype lose their ability to adhere onto basolateral membranes, instead obtaining the mesenchymal phenotype, which can readily migrate and invade [23]. This allows them to detach from the primary tumor, enter the circulation and metastasize to distant sites [23]. Therefore, exploring the under-

lying mechanism of the EMT process may improve the diagnosis and therapeutic strategies against tumor invasion and metastasis. Previous studies demonstrated that OMT treatment can alleviate or even reverse the EMT process *in vitro*. Guo *et al.* [24] previously found that OMT can inhibit the cancer-associated fibroblasts of hepatocellular carcinoma by reversing EMT *in vitro*. In another study, Chen *et al.* [25] also reported that OMT treatment reversed the EMT process in breast cancer cells. In this study, we found that OMT treatment can suppress irradiation-induced EMT, invasion and migration in NSCLC cells through the DcR3/AKT/GSK-3 $\beta$  pathway *in vitro*. Therefore, inhibiting the EMT process by OMT treatment may serve as a novel method for prevent the metastasis of NSCLC.

DcR3 is a member of the TNFR superfamily. Previous articles reported that DcR3 can inhibit apop-





tosis, induce angiogenesis and modulate immune cell function [26]. Therefore, DcR3 may also serve a key role in the pathogenesis of various malignancies. Ge *et al.* [16] found that DcR3 can induce the proliferation, migration and invasion of gas-

tric cancer cells by promoting EMT. In this study, we demonstrated that OMT treatment inhibited DcR3 activation to suppress irradiation-induced EMT, invasion and migration in NSCLC cells, which restored radiosensitivity *in vitro*. Furthermore, it

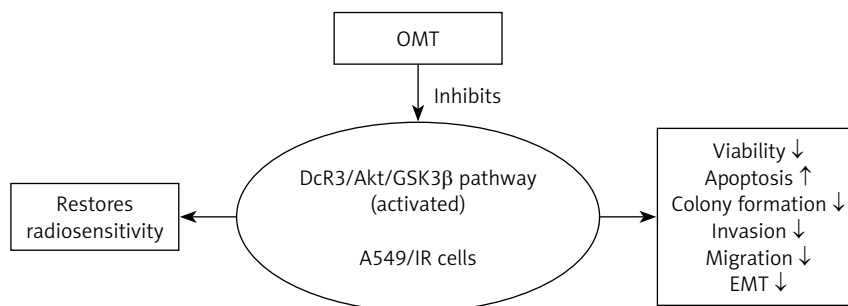


**Figure 13.** The DcR3/AKT/GSK-3 $\beta$  pathway was activated in radioresistant A549 cells, but OMT suppressed the development of radioresistance in A549 cells (decreasing the viability, colony formation, invasion, migration and EMT, while increasing apoptosis) by inhibiting the DcR3/AKT/GSK-3 $\beta$  pathway (Figure 11)

*DcR3* – decoy receptor 3, *OMT* – oxymatrine, *Akt* – protein kinase B, *GSK-3 $\beta$*  – glycogen synthase kinase 3 $\beta$ , *EMT* – epithelial-mesenchymal transition, *A549/IR cells* – radioresistant A549 cells.

was revealed that the DcR3/AKT/GSK-3 $\beta$  pathway was important for the survival and EMT of radioresistant NSCLC cells (Figure 8). There was no previous study about the effect of OMT on DcR3, but some studies have shown the possible regulation of OMT on AKT/GSK-3 $\beta$  pathway. Liu et al revealed that Oxymatrine protects neonatal rat against hypoxic-ischemic brain damage via PI3K/Akt/GSK3 $\beta$  pathway [27]. Another study found that oxymatrine attenuates brain hypoxic-ischemic injury from apoptosis and oxidative stress via the Akt/GSK3 $\beta$ /HO-1/Nrf-2 signaling pathway [28]. In addition, PI3K/Akt/GSK-3 $\beta$  signaling was also found to be involved in the effect of effect of oxymatrine on hepatocyte apoptosis [29]. The AKT signaling pathway has been previously reported to be activated in other types of cancer and was therefore proposed to be a potential target for cancer treatment [30]. As a component of this essential intracellular signaling pathway, AKT serves an important role in maintaining cell survival and growth, especially during cancer progression and radioresistance induction [31]. Therefore, it may be a valuable strategy to target tumors by inhibiting AKT activation. A number of studies have reported that AKT signaling may serve as one of downstream targets of DcR3. Chen *et al.* [32] showed that DcR3 can regulate inflammation and apoptosis through the PI3K/AKT signaling pathway in coronary heart disease. Additionally, AKT signaling has also been found to be an upstream effector of GSK3 $\beta$ . Ge *et al.* [16] found that DcR3 can also promote the proliferation of gastric cancer through the AKT/GSK-3 $\beta$  pathway *in vitro*. In addition, ham *et al.* [33] reported that saechalssal may reduce blood glucose in diabetic mice by modulating the AKT/GSK-3 $\beta$  pathway. In this study, we identified AKT/GSK-3 $\beta$  as the downstream pathway of DcR3 and showed that this form of DcR3/AKT signaling was activated in radioresistant NSCLC cells. DcR3 was shown to activate the expression of some com-

ponents of the PI3K/AKT/GSK-3 $\beta$ / $\beta$ -catenin signaling pathway, such as p-AKT, GSK-3 $\beta$ , p-GSK-3 $\beta$  and  $\beta$ -catenin [16]. The knockdown of DcR3 led to decreased expression of p-AKT, GSK-3 $\beta$ , p-GSK-3 $\beta$ , and  $\beta$ -catenin in hGC27 and MKN28 cells, indicating that DcR3 was an upstream regulator of AKT/GSK-3 $\beta$  pathway. This result is consistent with our study. Interestingly, our study demonstrated that the DcR3/AKT/GSK-3 $\beta$  pathway was involved in radioresistance. A previous study showed that Dcr3 expression was higher in h1299 cells than h460 cells [34]. The Dcr3 mRNA expression level in the radioresistant cell lines was increased, and overexpression of Dcr3 increased the survival rate of radiosensitive h460, MCF7, and U87MG cells, while knockdown of Dcr3 abolished the radioresistance of A549 cells [34]. Combined with our study, these results showed that Dcr3 may be an important molecule in the regulation of radioresistance of lung cancer cells. Numerous studies have suggested the involvement of AKT/GSK-3 $\beta$  pathway in radioresistance [35–38]. Using the AKT inhibitor MK-2206, we revealed that the inhibition of AKT/GSK-3 $\beta$  pathway was responsible for the effect of OMT on radiosensitivity.

Previous studies found that OMT can mediate its function in various physiological and pathological processes through the AKT signaling pathway, including liver gluconeogenesis, breast cancer, hypoxic-ischemic brain damage and cardiomyocyte injury [39–42]. Our *in vitro* experiments also support the hypothesis that OMT treatment can restore radiosensitivity to inhibit irradiation-induced EMT, invasion and migration in NSCLC cells through the DcR3/AKT/GSK-3 $\beta$  pathway. These findings suggest that the DcR3/AKT/GSK-3 $\beta$  pathway may become a potential therapeutic target for OMT treatment in NSCLC in the future.

In conclusion, to the best of our knowledge our study was the first to reveal a protective impact of OMT treatment in radioresistant NSCLC.

This study also demonstrated that the DcR3/AKT/GSK-3 $\beta$  axis was activated in radioresistant NSCLC cells. OMT treatment was found to restore radio-sensitivity and inhibited irradiation-induced EMT, invasion and migration in NSCLC cells by inhibiting the DcR3/AKT/GSK-3 $\beta$  pathway *in vitro*. In addition, OMT treatment promoted the inhibitory effects of radiation on tumor growth in radioresistant xenograft models (Figure 13). Therefore, these findings may be beneficial for deepening the understanding into the effects of OMT treatment on radioresistance and EMT in NSCLC. These results indicated that OMT may be developed to be a medicine against radioresistance and EMT in NSCLC, and the DcR3/AKT/GSK-3 $\beta$  may be targeted when we want to explore new medicines in NSCLC therapy. However, there are still several limitations in the present study. First, the exact mechanism of OMT on DcR3/AKT/GSK-3 $\beta$  pathway needs further study. Second, we only performed cell and animal experiments. The clinical study was absent, which can be performed in the near future to confirm the effect of OMT in clinical settings.

### Conflict of interest

The authors declare no conflict of interest.

### References

- Baker MJ, Cooke M, Kazanietz MG. Nuclear PKC $\alpha$  and ribosome biogenesis: A novel axis in lung tumorigenesis. *Cancer Cell* 2017; 31: 167-9.
- Liu Y, Feng X, Kang S, Lv F, Ni Y, Wu H. CircRIP2 promotes NSCLC progression by sponging for miR-671-5p to regulate FOXM1 expression. *histol histopathol* 2022; 37: 117-24.
- Evison M; AstraZeneca UK Limited. The current treatment landscape in the UK for stage III NSCLC. *Br J Cancer* 2020; 123 (Suppl. 1): 3-9.
- Zhang YY, Yi M, Huang YP. Oxymatrine ameliorates doxorubicin-induced cardiotoxicity in rats. *Cell Physiol Biochem* 2017; 43: 626-35.
- Li W, Yu X, Tan S, Liu W, Zhou L, Liu H. Oxymatrine inhibits non-small cell lung cancer via suppression of EGFR signaling pathway. *Cancer Med* 2018; 7: 208-18.
- Yu Q, Luo J, Zhang J, et al. Oxymatrine inhibits the development of non-small cell lung cancer through miR-367-3p upregulation and target gene SGK3 downregulation. *Am J Transl Res* 2020; 12: 5538-50.
- Zhu HF, Liu YP, Liu DL, et al. Role of TGF $\beta$ 3-Smads-Sp1 axis in DcR3-mediated immune escape of hepatocellular carcinoma. *Oncogenesis* 2019; 8: 43.
- Lagou S, Grapsa D, Syrigos N, Bamias G. The role of decoy receptor DcR3 in gastrointestinal malignancy. *Cancer Diagn Progn* 2022; 2: 411-21.
- Lin WW, Hsieh SL. Decoy receptor 3: a pleiotropic immunomodulator and biomarker for inflammatory diseases, autoimmune diseases and cancer. *Biochem Pharmacol* 2011; 81: 838-47.
- Zhang Y, Luo J, He R, et al. Expression and clinicopathological implication of DcR3 in lung cancer tissues: a tissue microarray study with 365 cases. *Onco Targets Ther* 2016; 9: 4959-68.
- Ying C, Wang S, Lu Y, et al. Glucose fluctuation increased mesangial cell apoptosis related to AKT signal pathway. *Arch Med Sci* 2019; 15: 730-7.
- Li W, Huang X, Bi D. miRNA-21 plays an important role in necrotizing enterocolitis. *Arch Med Sci* 2019; 18: 406-12.
- Lambert AW, Pattabiraman DR, Weinberg RA. Emerging biological principles of metastasis. *Cell* 2017; 168: 670-91.
- Roche J. The epithelial-to-mesenchymal transition in cancer. *Cancers* 2018; 10: 79.
- Zhang H, Chen X, Li D, et al. DcR3 promotes hepatoma cell migration by downregulating E-cadherin expression. *Oncol Rep* 2017; 38: 377-83.
- Ge H, Liang C, Li Z, et al. DcR3 induces proliferation, migration, invasion, and EMT in gastric cancer cells via the PI3K/AKT/GSK-3 $\beta$ / $\beta$ -catenin signaling pathway. *Onco Targets Ther* 2018; 11: 4177-87.
- Hanna NH, Schneider BJ, Temin S, et al. Therapy for stage IV non-small-cell lung cancer without driver alterations: ASCO and OH (CCO) joint guideline update. *J Clin Oncol* 2020; 38: 1608-32.
- Tan DS, Leighl NB, Riely GJ, et al. Safety and efficacy of naxartinib (EGF816) in adults with EGFR-mutant non-small-cell lung carcinoma: a multicentre, open-label, phase 1 study. *Lancet Respir Med* 2020; 8: 561-72.
- Zhou R, Xu Q, Xu Y, Xiong A, Wang Y, Ma P. Oxymatrine attenuated isoproterenol-induced heart failure in rats via regulation of COX-2/PDGFR pathway. *Biomed Pharmacother* 2016; 84: 1359-66.
- Dai JP, Wang QW, Su Y, et al. Oxymatrine inhibits influenza A virus replication and inflammation via TLR4, p38 MAPK and NF- $\kappa$ B pathways. *Int J Mol Sci* 2019; 19: 965.
- Huang Y, Li X, Zhang X, Tang J. Oxymatrine ameliorates memory impairment in diabetic rats by regulating oxidative stress and apoptosis: involvement of NOX2/NOX4. *Oxid Med Cell Longev* 2020; 2020: 3912173.
- Siegel RL, Miller KD, Jemal A. Cancer statistics, 2020. *Cancer J Clin* 2020; 70: 7-30.
- Brabletz T, Kalluri R, Nieto MA, Weinberg RA. EMT in cancer. *Nat Rev Cancer* 2018; 18: 128-34.
- Guo J, Zeng H, Shi X, et al. A CFH peptide-decorated liposomal oxymatrine inactivates cancer-associated fibroblasts of hepatocellular carcinoma through epithelial-mesenchymal transition reversion. *J Nanobiotechnology* 2022; 20: 114.
- Chen Y, Chen L, Zhang JY, et al. Oxymatrine reverses epithelial-mesenchymal transition in breast cancer cells by depressing  $\alpha_v\beta_3$  integrin/FAK/PI3K/Akt signaling activation. *Onco Targets Ther* 2019; 12: 6253-65.
- Zhong M, Qiu X, Liu Y, et al. TIPE regulates DcR3 expression and function by activating the PI3K/AKT signaling pathway in CRC. *Front Oncol* 2021; 10: 623048.
- Liu Y, Wang H, Liu N, et al. Oxymatrine protects neonatal rat against hypoxic-ischemic brain damage via PI3K/Akt/GSK3 $\beta$  pathway. *Life Sci* 2020; 254: 116444.
- Ge XH, Shao L, Zhu GJ. Oxymatrine attenuates brain hypoxic-ischemic injury from apoptosis and oxidative stress: role of p-Akt/GSK3 $\beta$ /HO-1/Nrf-2 signaling pathway. *Metab Brain Dis* 2018; 33: 1869-75.
- Zhang X, Jiang W, Zhou AL, Zhao M, Jiang DR. Inhibitory effect of oxymatrine on hepatocyte apoptosis via TLR4/PI3K/Akt/GSK-3 $\beta$  signaling pathway. *World J Gastroenterol* 2017; 23: 3839-49.
- Mundi PS, Sachdev J, McCourt C, Kalinsky K. AKT in cancer: new molecular insights and advances in drug development. *Br J Clin Pharmacol* 2016; 82: 943-56.

31. Mayer IA, Arteaga CL. The PI3K/AKT pathway as a target for cancer treatment. *Annu Rev Med* 2016; 67: 11-28.
32. Chen X, Wang R, Chen W, Lai L, Li Z. Decoy receptor-3 regulates inflammation and apoptosis via PI3K/AKT signaling pathway in coronary heart disease. *Exp Ther Med* 2019; 17: 2614-22.
33. Ham JR, Son YJ, Lee Y, et al. Korean naked waxy barley (saechalssal) extract reduces blood glucose in diabetic mice by modulating the PI3K-Akt-GSK3 $\beta$  pathway. *Biomed Pharmacother* 2022; 150: 112976.
34. Sung hY, Wu hG, Ahn JH, Park WY. Dcr3 inhibit p53-dependent apoptosis in gamma-irradiated lung cancer cells. *Int J Radiat Biol* 2010; 86: 780-90.
35. Yang XX, Ma M, Sang MX, Zhang XY, Zou NY, Zhu SC. Knockdown of FAM83D enhances radiosensitivity in coordination with irradiation by inhibiting EMT via the Akt/GSK-3 $\beta$ /Snail signaling pathway in human esophageal cancer cells. *Onco Targets Ther* 2020; 13: 4665-78.
36. Wang h, Wang Z, Li Y, Lu T, hu G. Silencing snail reverses epithelial-mesenchymal transition and increases radiosensitivity in hypopharyngeal carcinoma. *Onco Targets Ther* 2020; 13: 497-511.
37. Zhang W, Li L, Guo E, et al. Inhibition of PDK1 enhances radiosensitivity and reverses epithelial-mesenchymal transition in nasopharyngeal carcinoma. *head Neck* 2022; 44: 1576-87.
38. Zuo Z, Ji S, he L, Zhang Y, Peng Z, han J. LncRNA TTN-AS1/miR-134-5p/PAK3 axis regulates the radiosensitivity of human large intestine cancer cells through the P21 pathway and AKT/GSK-3 $\beta$ / $\beta$ -catenin pathway. *Cell Biol Int* 2020; 44: 2284-92.
39. Zhu YX, hu hQ, Zuo ML, et al. Effect of oxymatrine on liver gluconeogenesis is associated with the regulation of PEPCK and G6Pase expression and AKT phosphorylation. *Biomed Rep* 2021; 15: 56.
40. Guo L, Yang T. Oxymatrine inhibits the proliferation and invasion of breast cancer cells via the PI3K pathway. *Cancer Manag Res* 2019; 11: 10499-508.
41. Wei W, Lu M, Lan XB, et al. Neuroprotective effects of Oxymatrine on PI3K/Akt/mTOR pathway after hypoxic-ischemic brain damage in neonatal rats. *Front Pharmacol* 2021; 12: 642415.
42. Zhang Z, Qin X, Wang Z, et al. Oxymatrine pretreatment protects h9c2 cardiomyocytes from hypoxia/reoxygenation injury by modulating the PI3K/Akt pathway. *Exp Ther Med* 2021; 21: 556.